Siphonophore Phylogeny

Stefan Siebert[1,2], Felipe Zapata[1,3], Mark Howison[4], Cat Munro[1], Alejandro Damian Serrano[1], Samuel H Church^1, 5^, Freya Goetz[1,5], Phil Pugh, Steven H.D. Haddock[4], Casey W. Dunn[1]*

[1] Department of Ecology and Evolutionary Biology, Brown University, Providence, RI, USA

[2] Current address: Department of Molecular & Cellular Biology, University of California at Davis, Davis, CA, USA

[3] Current address: Department of Ecology and Evolutionary Biology, University of California Los Angeles, Los Angeles, CA, USA

[4] Brown Data Science Practice, Brown University, Brown University, Providence, RI, USA

[5] Harvard

[5] Current address: Smithsonian, Washington DC, USA

[4] Monterey Bay Aquarium Research Institute, Moss Landing, CA, USA

* Corresponding author, casey_dunn@brown.edu

Abstract

Introduction

Siphonophores are...

Methods

This manuscript is an executable document computed directly from the data, providing an explicit and reproducible description of all findings. All scripts for the analyses are available in a git repository at https://github.com/caseywdunn/siphonophore_phylogeny_2017. The most recent commit at the time of the analysis presented here was 1800831f2de62548d149e6f6347387893c6d8a48.

Collecting

Collection data on all examined specimens, a description of the tissue that was sampled from the colony, collection mode, sample processing details, mRNA extraction methods, sequencing library preparation methods and sequencing details are summarized in supplementary table 1. Monterey Bay and Gulf of California specimens were collected by remotely operated underwater vehicle (ROV) or during blue-water scuba dives. *Chelophyes appendiculata* and *Hippopodius hippopus* specimens were collected in the bay of Villefranche-sur-Mer, France, during a plankton trawl on 04/13/11. Available physical vouchers have been deposited at the Museum of Comparative Zoology (Harvard University), Cambridge, MA, and at the United States National Museum (Smithsonian Institution), Washington, DC. Accession numbers are given in supplementary table X. In cases where physical vouchers were unavailable we provide photographs to document species identity (table x).

Sequencing

When possible specimens were starved overnight in filtered seawater at temperatures close to ambient water temperatures at the time point of specimen collection (supplementary table 1). mRNA was extracted directly from tissue using a variety of methods (supplementary table x): Magnetic mRNA Isolation Kit (NEB, #S1550S), Invitrogen Dynabeads mRNA Direct Kit (Ambion, #61011), Qymo Quick RNA MicroPrep (Zymo

#R1050), or from total RNA after Trizol (Ambion, #15596026) extraction and through purification using Dynabeads mRNA Purification Kit (Ambion, #61006)- in case of very small total RNA quantities, only a single round of bead purification was performed; or Trizol directly into the Illumina TruSeq Stranded Library Kit. Extractions were performed according to the manufacturer's instruction. Any resulting higher rRNA read counts were dealt with further downstream in the bioinformatics workflow. Libraries were prepared for sequencing using the Illumina TruSeq RNA Sample Prep Kit (Illumina, #FC-122-1001, #FC-122-1002), the Illumina TruSeq Stranded Library Prep Kit (Illumina, #RS-122-2101) or the NEBNext RNA Sample Prep Master Mix Set (NEB, #E6110S). We collected long read paired end Illumina data for *de novo* transcriptome assembly.In the case of large tissue inputs, libraries were sequenced separately for each tissue and subsequently were subsampled and pooled *in silico*. Libraries were sequenced on the HiSeq 2000, 2500, and 3000 sequencing platforms (supplementary table 1). Summary statistics for expression libaries are given in Table 1.

Analysis

New data were analysed in conjunction with 13 publically available datasets, with a total number of 43 species. Sequence assembly, annotation, Maximum Likelihood (ML) phylogenetic analysis were conducted with the tool Agalma (Dunn et al. 2013), v. 1.00, and Bayesian Inference (BI) analyses were conducted using Phylobayes(Lartillot et al. 2009) v. 1.7a-mpi. Source code for all analysis steps, sequence alignments, sampled and consensus trees, and voucher information are available in a git repository https://github.com/caseywdunn/siphonophore_phylogeny_2017.

In the final analyses, we sampled 1,071 genes to generate a supermatrix with 60% occupancy and a length of 378,468 amino acids. Two outgroup species, *Atolla vanhoeffeni* and *Aegina citrea*, were removed from the final supermatrix and phylogeny due to low gene occupancy (gene sampling of 20.8% and 14.5% respectively in a 50% occupancy matrix with 2,203 genes). ML analyses were conducted on the unpartitioned supermatrix using the WAG+Γ model of amino acid substitution, and bootstrap values were estimated using 1000 replicates. BI was conducted using two different CAT models, CAT-Poisson and CAT-GTR (Lartillot and Philippe 2004). Two independent MCMC chains were run under the CAT-GTR model, and four independent MCMC chains were run under the CAT-Poisson model. The CAT-GTR and CAT-poisson models did not converge after a long CPU time, and only the results from the CAT-poisson model are included here.

Subsequent analyses were conducted in R and integrated into this manuscript with the `knitr` package. See Supplementary Information for R package version numbers.

Hypothesis testing

Results and Discussion

Sample collecting and sequencing

% latex table generated in R 3.4.1 by xtable 1.8-2 package % Mon Oct 30 15:31:43 2017

Table 1 (at the end of file): Summary statistics for libraries.

Species phylogeny

(XX This paragraph on sampling through Agalma analyses) The analyses presented here consider XXX siphonophore species and 8 outgroup species. This includes new data for XXX species. Summary stats on assemblies XX (Table XX). Matrix has XX genes, XX sites, and occupancy is XX.

(XX This paragraph on summarizes phylogeny runs, apart from tree topology) Maximimum likelihood analyses had 1000 replicates. We ran 4 phylobayes chains, and visual inspection of the traces indicated that a burn in of 400 trees was sufficient for all runs. This left 15847 trees in the posterior. XXConvergence...

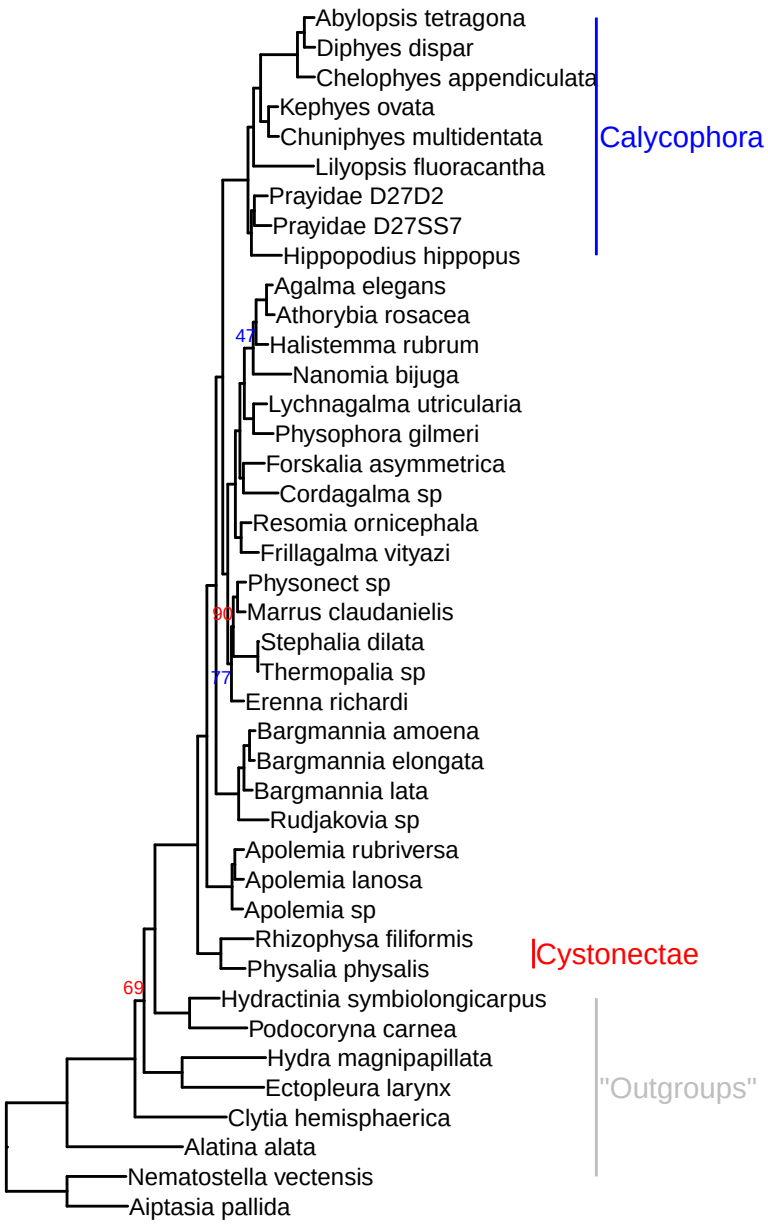

Figure 1: Phylogram of siphonophore relationships. Node labels indicate bootstrap support percent, unnumbered nodes have 100% support. The image was rendered with ggtree (Yu et al. 2016)

These findings are entirely consistent with a previous analysis based on two genes (16S and 18S ribosomal RNA) (Dunn et al. 2005). Cystonectae is the sister group to the remaining siphonophores, and Calycophorae is nested within the paraphyletic "Physonectae". In addition, multiple nodes that were not resolved in the previous two-gene analysis do recieve strong support in this 1,071-gene transcriptome analysis. These findings include XXX.

Character Evolution

Siphonohores have evolved a fascinating diversity of morphological features, zooid types, life history traits, and habitats. Here we explore the evolutionary history of some of these features.

In our previous siphonophore phylogenetic analysis (Dunn et al. 2005) there were several characters left with equivocal evolutionary histories, due to unresolved relationships between physonects. With our current cladistic resolution, we were able to determine the following results:

Evolution of Monoecy

[Citation needed] noticed for the first time that some siphonophores were monoeicous and others were dioiecious. Our analyses in 2005 reconstructed this character and found a great amount of phylogenetic conservatism, with an unambiguous resolution of the MRCA as dioecious, and the appearance of monoecy in several taxa and clades (including Calycophorae) within the polytomy. Figure X shows the evolution of sex distribution in siphonophores under the current better-resolved tree model, and it strongly indicates that monoecy in siphonophores from a dioecious ancestor occured twice, in the branch leading to Calycophorae and in the branch leading to Agalmatids (sensu lato). There is a small probability for an alternative scenario featuring a single gain of monoecy before the split of Calycophorae, with a subsequent derived shift back to dioecy in the *Marrus-Erenna* clade.

The Evolution of Zooid Types

One of the most striking aspects of siphonophore biology is their diversity of unique zooid types. Other colonial cnidarians (such as Hydractinia) and some bryozoans (example) have been found to have up to X different zooid types [Citation1 , Citation 2]. The siphonophore genus Forskalia has 6 basic zooid types (pneumatophore, nectophore, gastrozooid, palpon, bract, and gonophore), and a total of 10 counting subtypes (4 types of bract, male & female gonophores). Diphyomorphs have more than 1 type of nectophore, while Cystonects have none. Here we reconstruct the evolutionary origins ofthe different zooid types and subtypes on the present transcriptome tree.

Nectophores are retained modified medusae Codonophora use for swimming. The nectosome is the region of the colony that develops from the nectosomal growth zone. Unlike the siphosomal growth zone, the nectosome does not bud gastrozooids, but nectophores (and in the case of *Apolemia*, also palpons). If fact, with the exception of *Physalia physalis* (which grows small nectophores near the gonodendra), siphonophore nectophores are exclusively found on the nectosome. It is likely that the MRCA of siphonophores had a nectosome, which has lost on the branch leading to Cystonects. We cannot exclude with certainty the alternative hypothesis of a nectosome-less ancestor followed by a gain of the nectosome in the branch leading to the Codonophora. The nectosome probably arose as a duplication of the siphosome, followed by functional specialization in propelling the colony. Figure X shows the origin of the dorsal nectosome in the Agalmatidae (sensu stricto) from an ancestral ventral nectosome.

All Codonophora have a nectosome, but the number and subtypes of nectophores present varies greatly between species. As shown in Figure X, most Codonophora presents the ancestral nectosome with multiple nectophores of the same subtype. However, Calycophorans evolved a different system with just 2 nectophores of one type. This shift may be associated with the loss of the pneumatophore. Not all Calycophorans remained with this arrangement. The Hippopodidae returned to bearing multiple identical nectophores, many

of which are inactive and serve functions of defense (like a shell to retract in) and buoyancy. As in the rest of Calycophorans, the Hippopodids only use 2 nectophores to propel the colony. Another interesting shift occurs in the branch leading to Diphyomorpha, where the 2 nectophores specialize into 2 subtypes, associated with a shift into a vertically aligned position and pointed bell shapes. The 2 types function together in a coupled hydrodynamic system that allows very fast escape responses (Mackie 1964).

Bracts also present a complex evolutionary history of subtypes (Figure X). Bracts are highly reduced zooids unique to siphonophores, but they are only present in the Codonophora. As with the nectosome, we have ambiguity determining whether the MRCA of siphonophores had bracts or not. The MRCA of Codonophora ahd only one bract subtype, which was lost in Hippopodidae and independently evolved into 2 subtypes in *Erenna* and *Nanomia*. During the branch leading to Forskalidae, bract subtypes evolved from 1 to 4 morphologically distinct forms. Bracts are important for protection of the delicate zooids and to help maintain neutral buoyancy. Some calycophorans are able to actively regulate the Na/NH4 balance to adjust their buoyancy (ref).

The ancestral siphonophore certainly had a pneumatophore (Figure X). This zooid type helps the colony float, maintain its pose, and regulate geotaxis (Church, 2013). Despite its diverse biological functions, it is lost in Calycophorae and never gained again in that clade. Calycophorans rely on the ionic balance of their gelatinous nectophores and bracts to retain posture and neutral buoyancy.

Palpons are modified mouthless gastrozooids used for digestion and circulation of the gastrovascular fluid. They were present in the MRCA of siphonophores (Figure X), retained in most species, but lost twice independently in the branches leading to *Bargmannia* and Calycophorae. These taxa must have found other avenues to effectively circulate nutrients across the colony.

The Gain and Loss of Tentilla

The most complex nematocyst batteries of Cnidaria can arguably be found among the siphonophores, hanging in regularly spaced tentacle side branches called tentilla. Most hydrozoans, including the clade that contains siphonophores, bear simple tentacles (tentacles with no side branches). Is is still an open question whether the most recent common ancestor (MRCA) of Siphonophora had simple or branched tentacles. The only two siphonophore genera regarded as lacking tentilla are *Physalia* and *Apolemia*, at each side of the earliest split in the siphonophore tree, with an immediate sister group with most members bearing tentilla (*Rhizophysidae* with the exception of *Bathyphysa conifera* and *{Bargmannia, Diphyes}*) (FigXX). Figure X shows the evolution of this character on the current phylogeny, indicating a most-likely tentilla bearing MRCA, with two independent losses. However, this reconstruction bears some uncertainty on the state of the MRCA, suggesting a ~30% probability of 2 independent gains of tentilla in the branches leading to *Rhizophysidae* and *{Bargmannia, Diphyes}*.

A key issue here is how we code for absence of tentilla, especially for the case of *Physalia physalis*. The tentacles of this species, when uncoiled, show very prominent, evenly spaced, 3D buttons which contain all active and functionally arranged nematocysts used by the organism for prey capture. Siphonophore tentilla are complete diverticular brachings of the tentacle ectoderm, mesoglea, and gastrovascular canal (lined by endoderm). Hessinger & Ford 1988 (in the Biology of Nematocysts) described these bands as enclosing individual fluid-filled chambers connected by narrow channels to the tentacular canal, lined by endoderm. This suggests they are not just ectodermal swellings, but probably are reduced tentilla. When we code *Physalia physalis* as tentilla bearing, the results for the character reconstraction change to a more parsimonious scenario (Figure X), indicating there was a single loss of tentilla in the branch leading to *Apolemiidae*. This result suggests an unambiguous tentilla-bearing state of the MRCA.

The Evolution of Vertical Habitat Use

Siphonophores are abundant predators in the pelagic realm, ranging from the surface (*Physalia physalis*) to bathypelagic depths (ref , *Bargmannia sp* 3888m VARS unpublished). While there are some pleustonic (*Physalia*) and benthic (*Rhodaliidae*) siphonophores, the phylogeny suggests the siphonophore MRCA was

planktonic, as most extant taxa are. Some interesting questions arise from these facts, including 1) what was the bathymetric niche of the siphonophore MRCA, and 2) how did siphonophore's vertical habitat use of the water columns evolve along the phylogeny. Our results indicate a mesopelagic MRCA, with several convergent transition events to epipelagic and bathypelagic waters. There was only a single transition to benthic lifestyle on the stem of *Rhodaliidae*.

Discussion

The strong phylogenetic signal in the characters traditinally used for taxonomic diagnostics is a positive indicator of the applicability and unambiguity of these characters.

Conclusions

Acknowledgements

This work was supported by the National Science Foundation (DEB-1256695 and the Waterman Award). Sequencing at the Brown Genomics Core facility was supported in part by NIH P30RR031153 and NSF EPSCoR EPS-1004057. Data transfer was supported by NSF RII-C2 EPS-1005789. Analyses were conducted with computational resources and services at the Center for Computation and Visualization at Brown University, supported in part by the NSF EPSCoR EPS-1004057 and the State of Rhode Island. We also thank the MBARI crews and ROV pilots for collection of the specimens.

Supplementary Information

Supplementary Analyses

The Tree

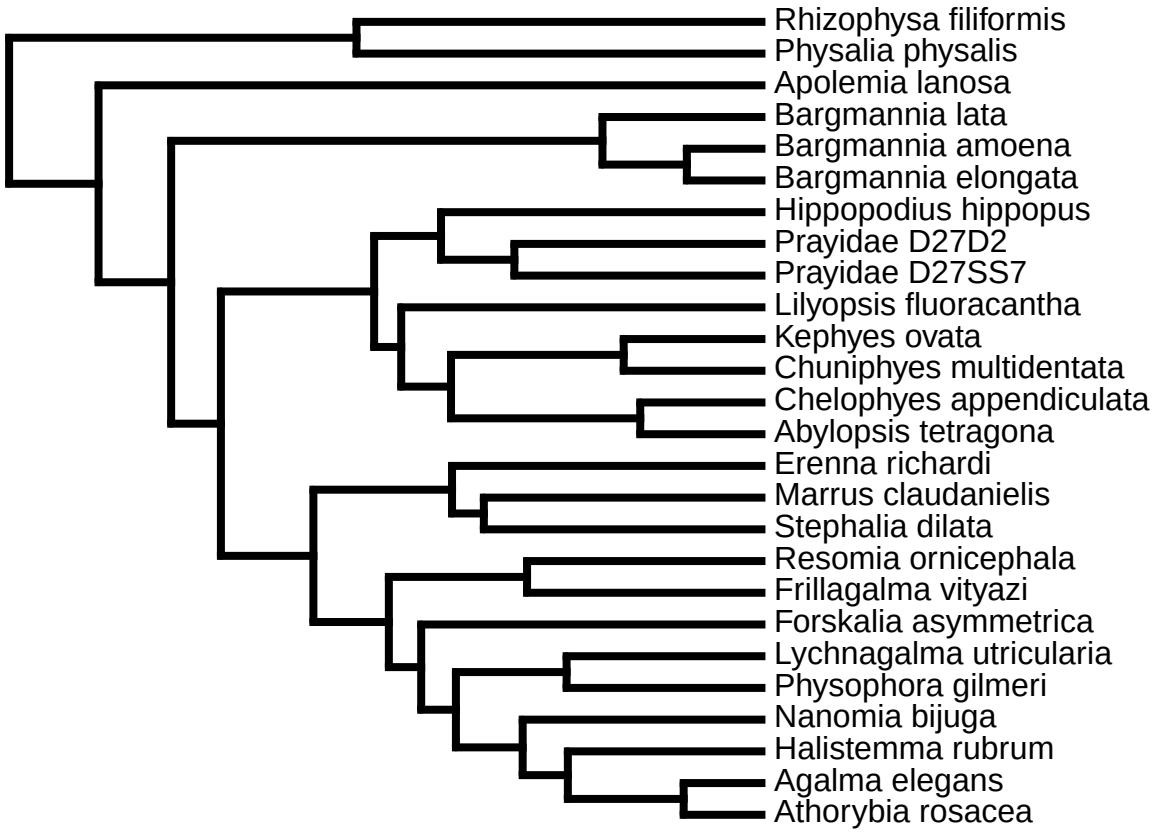

When we reconstruct the evolutionary history of different traits in siphonophore species, we obtain the following results:

SIMMAP Sex distribution

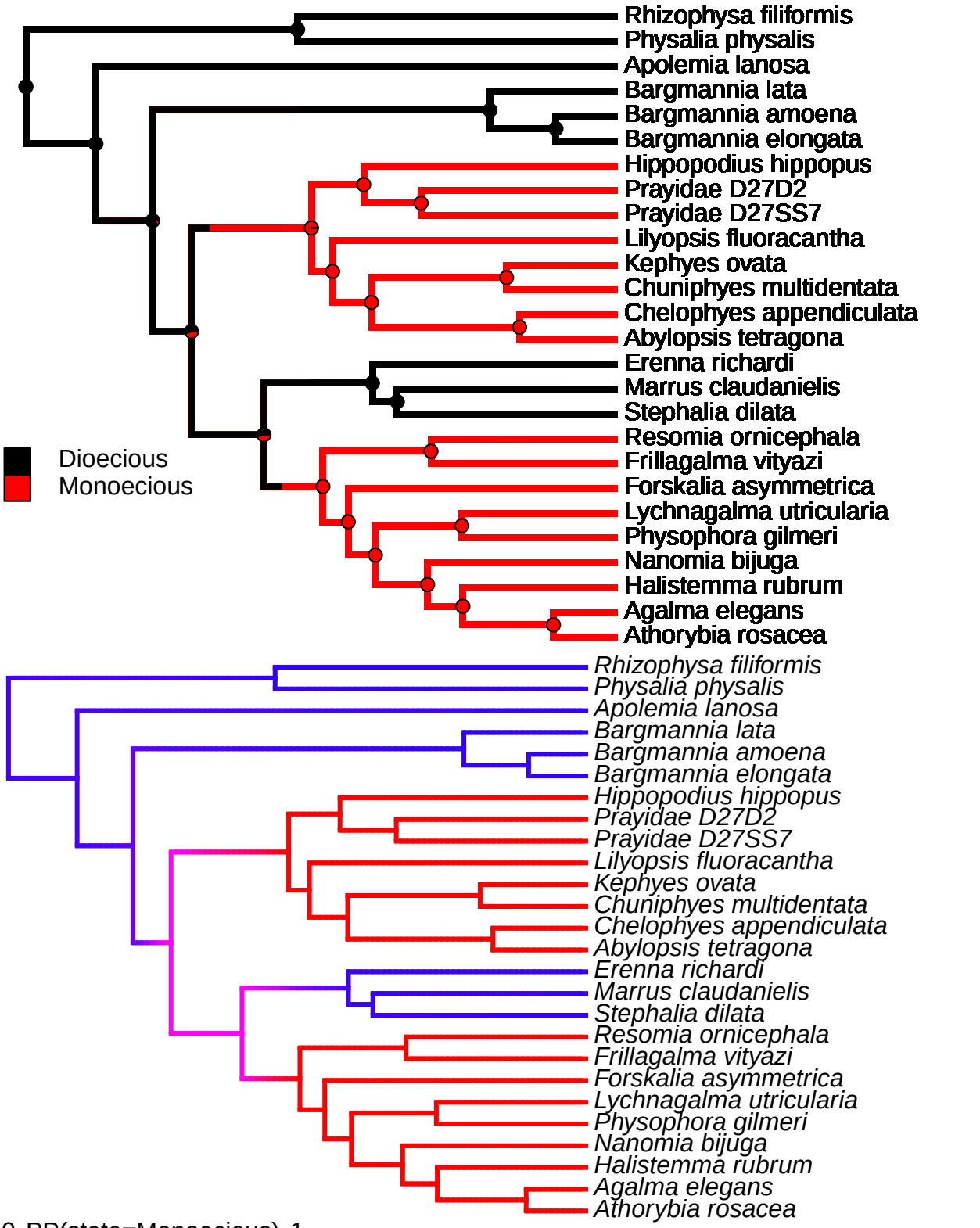

Posterior probabilities of states (0 Dioecious, 1 Monoecious).

SIMMAP Presence of palpons

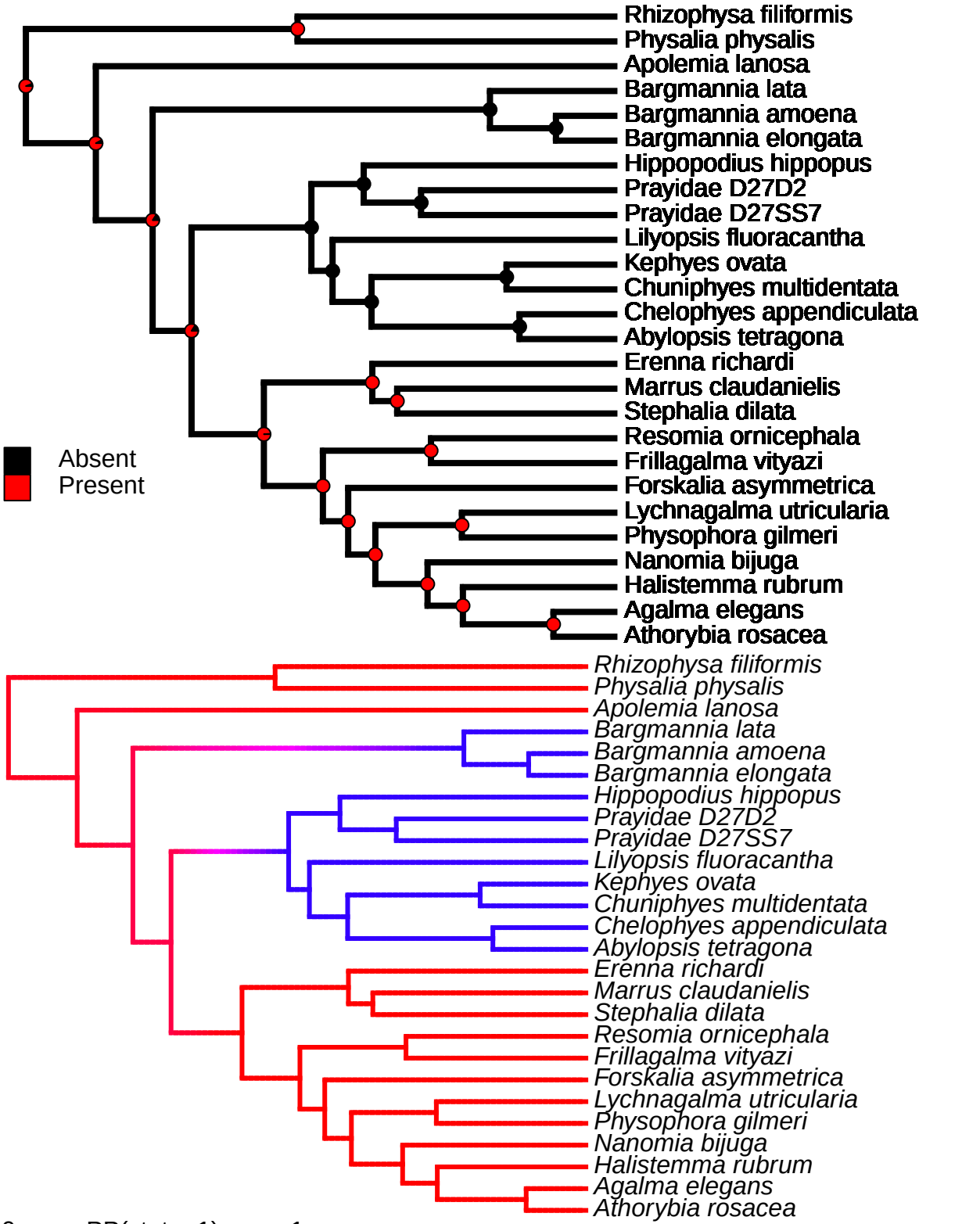

Posterior probabilities of states (1 Present, 0 Absent).

SIMMAP Presence of tentilla

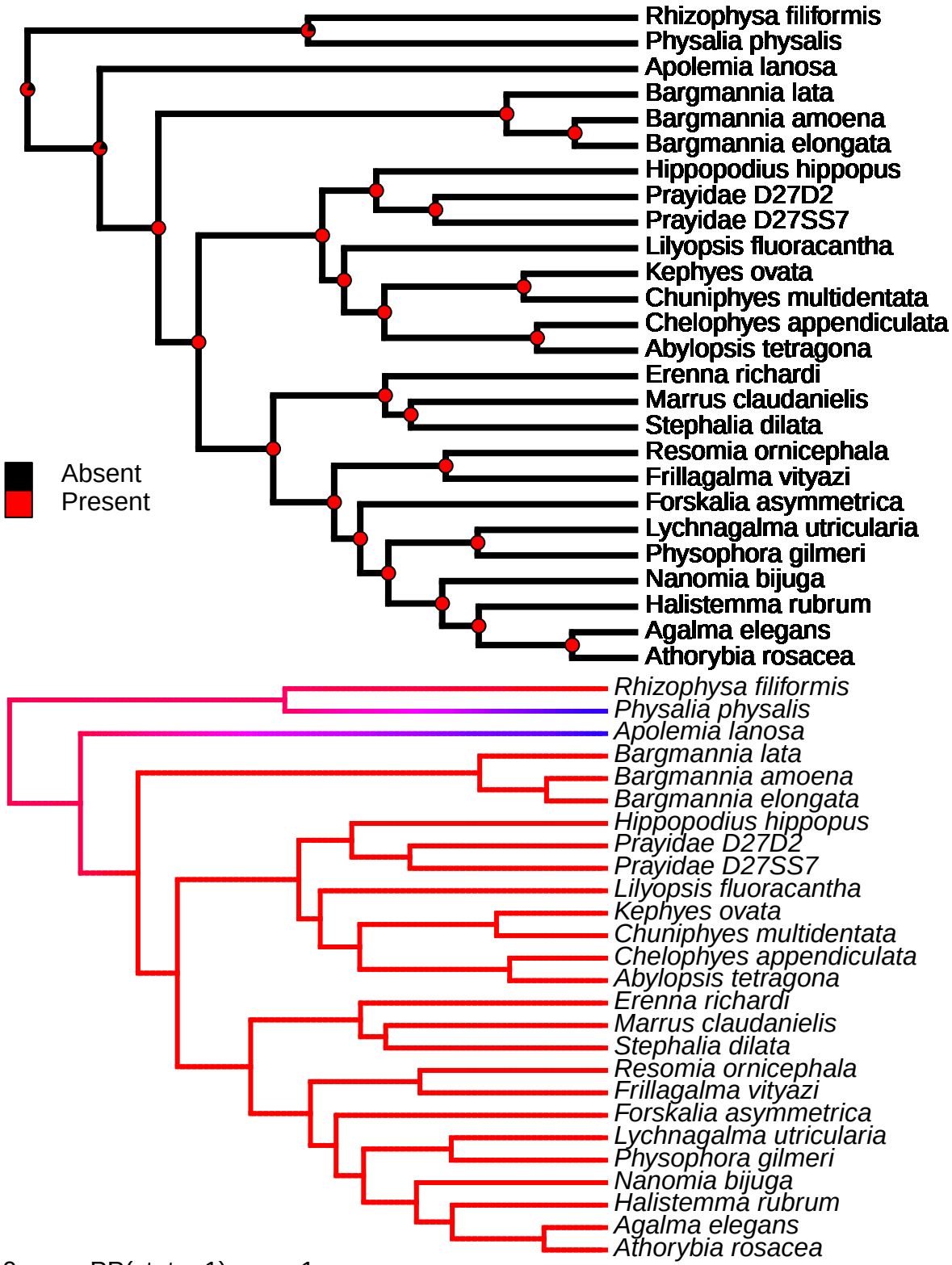

Posterior probabilities of states (1 Present, 0 Absent).

Physalia physalis may have reduced tentilla, which would indicate there was only one loss of tentilla at the branch leading to *Apolemia*.

SIMMAP Presence of tentilla - *Physalia* corrected

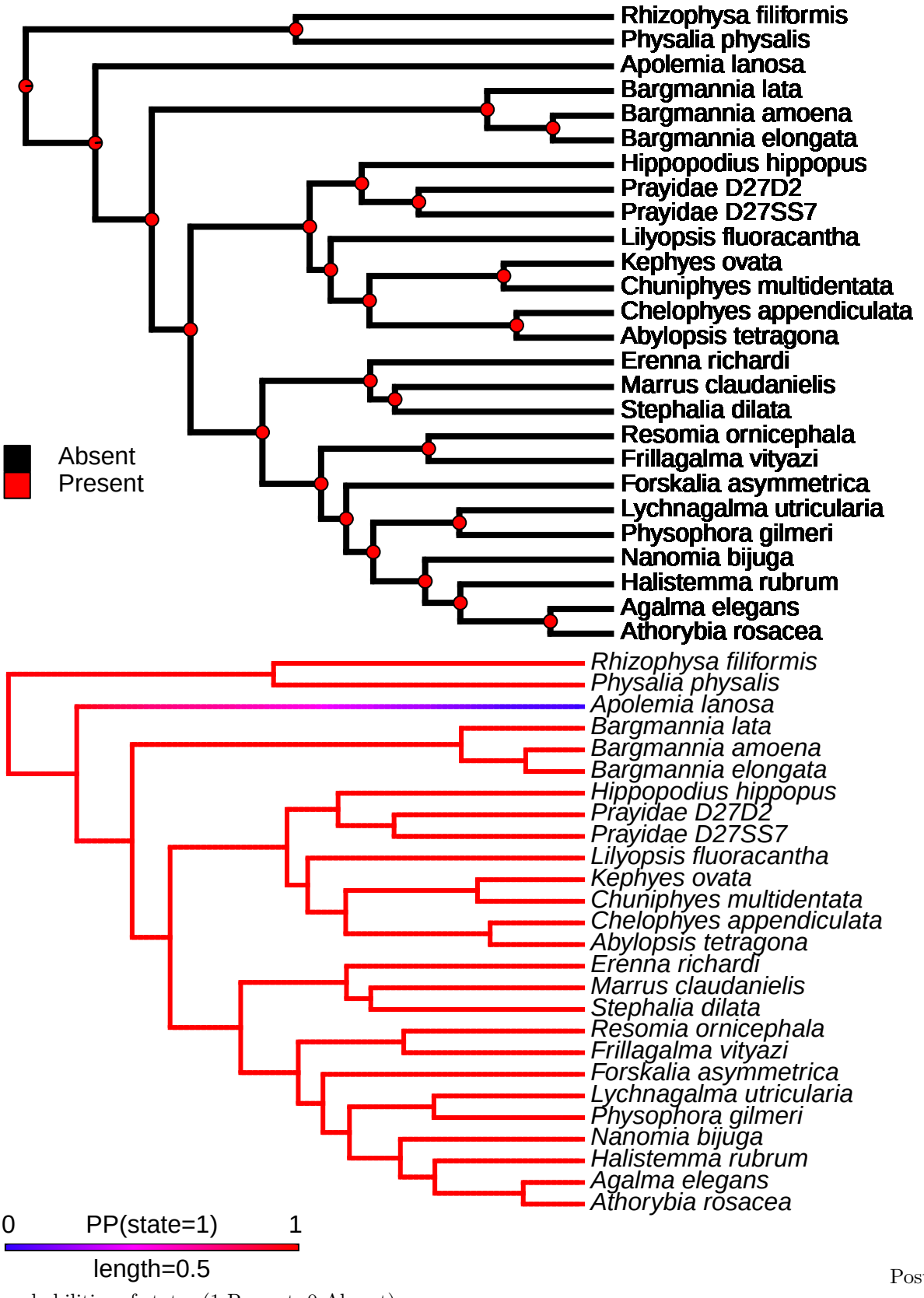

Posterior probabilities of states (1 Present, 0 Absent).

SIMMAP Presence of Nectophores

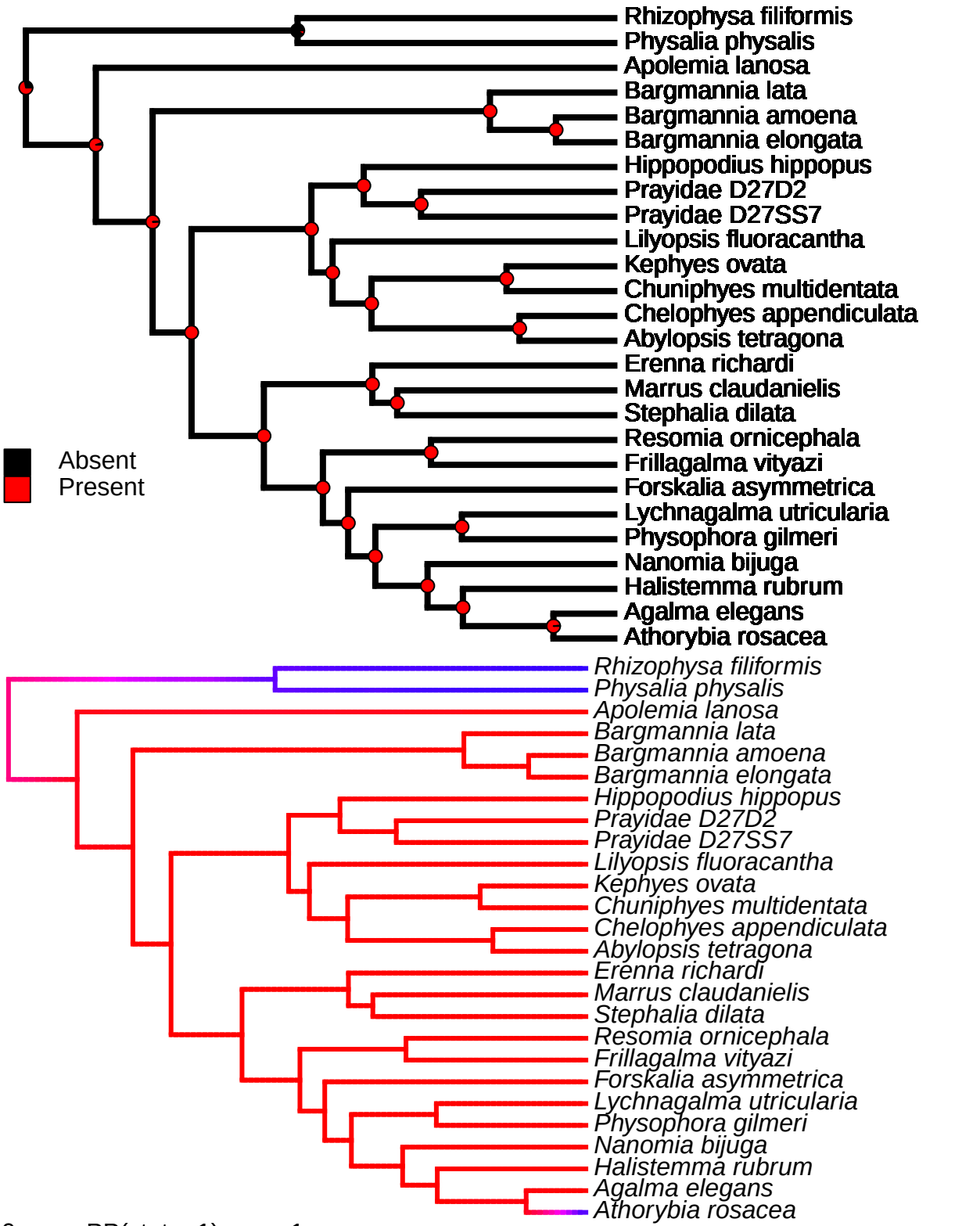

Posterior probabilities of states (1 Present, 0 Absent).

SIMMAP Position of Nectosome

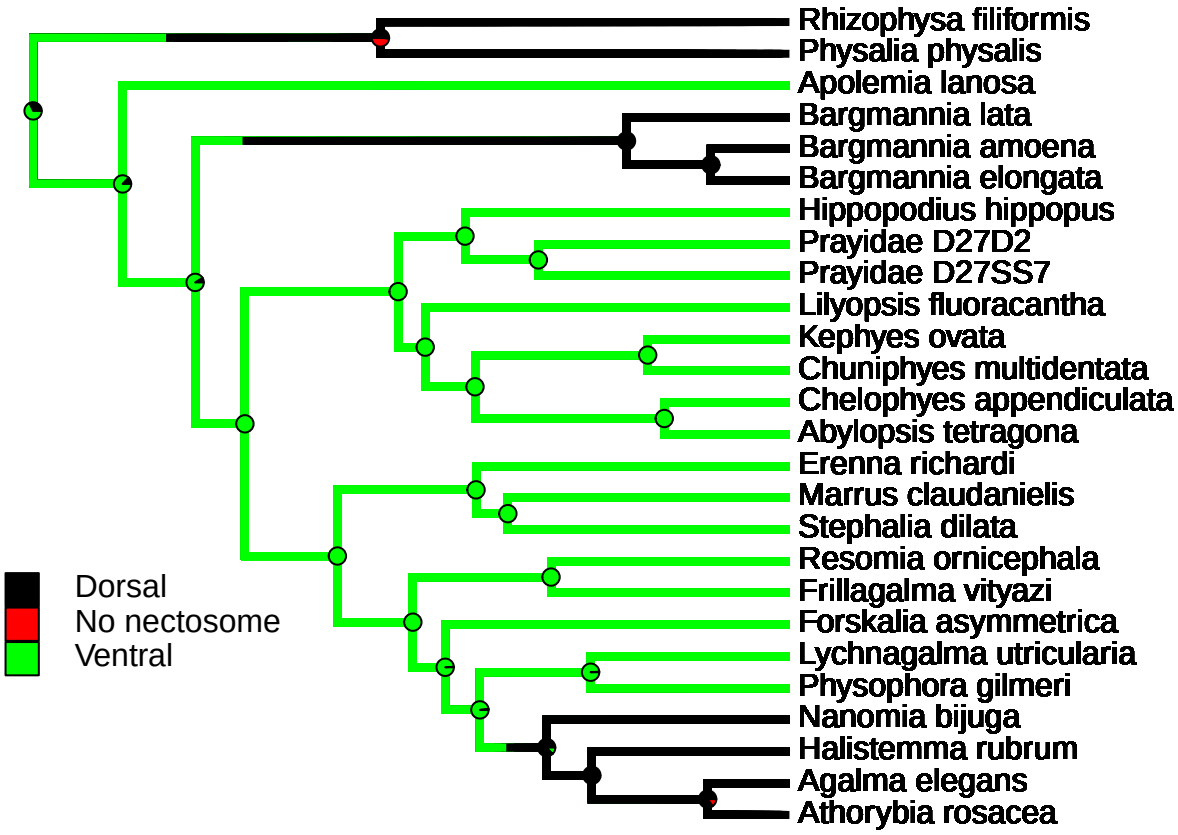

SIMMAP Nectophore number and types

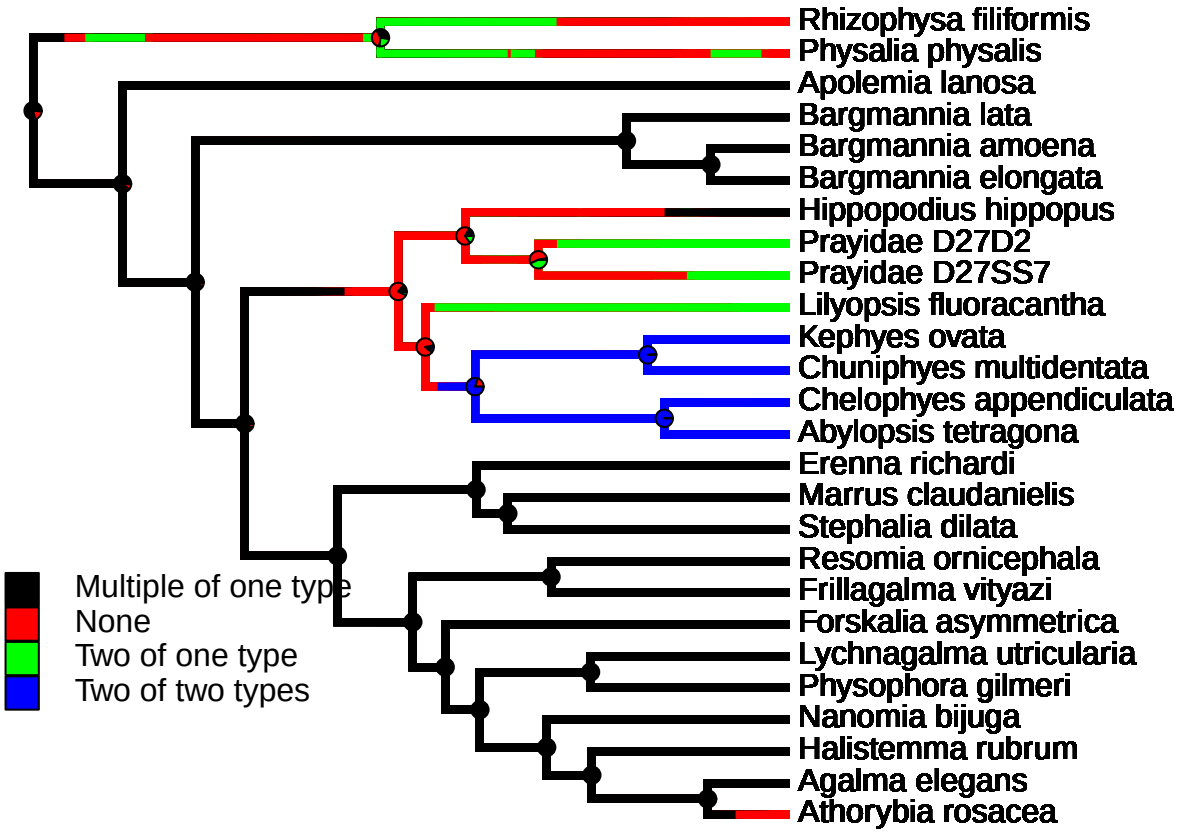

Posterior probabilities of states (1 Present, 0 Absent).It is not clear whether or not the stem group of siphonophores had a pneumatophore.

SIMMAP Habitat

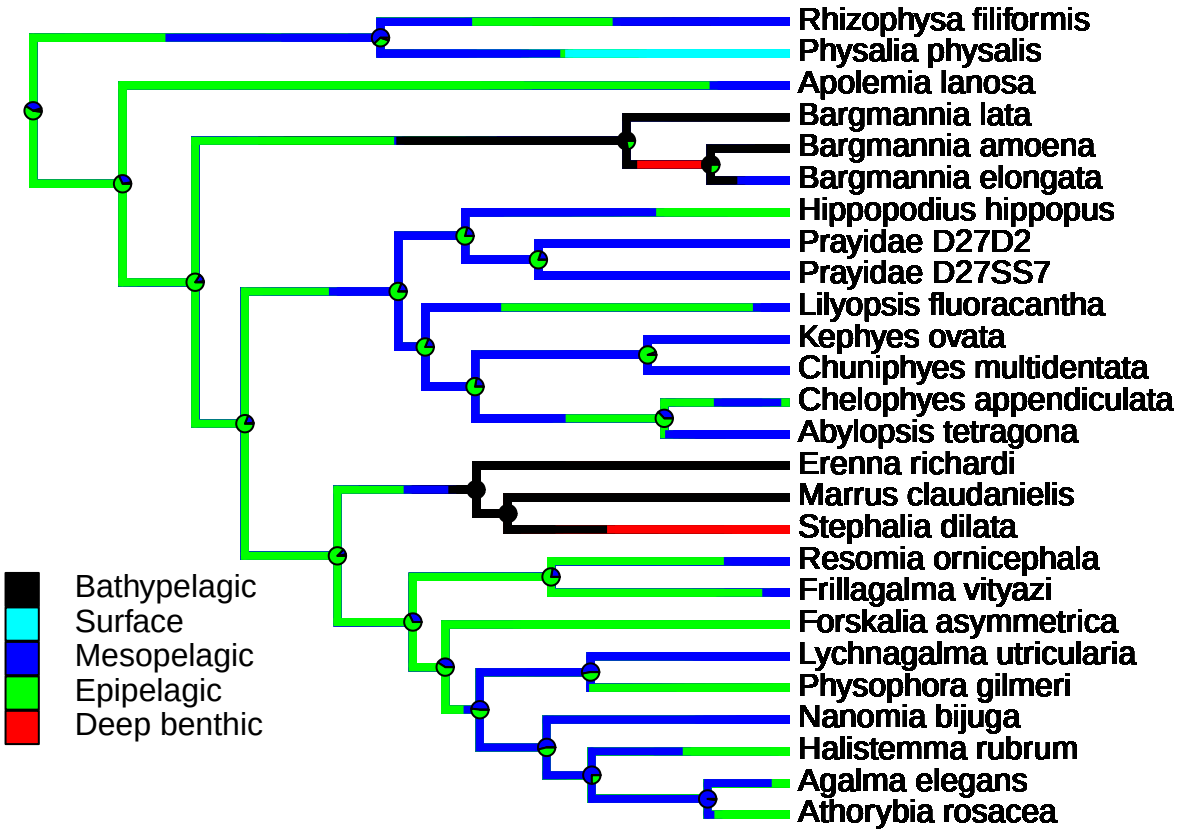

Continuous traits: Brownian motion reconstructions

Median depth reconstruction:

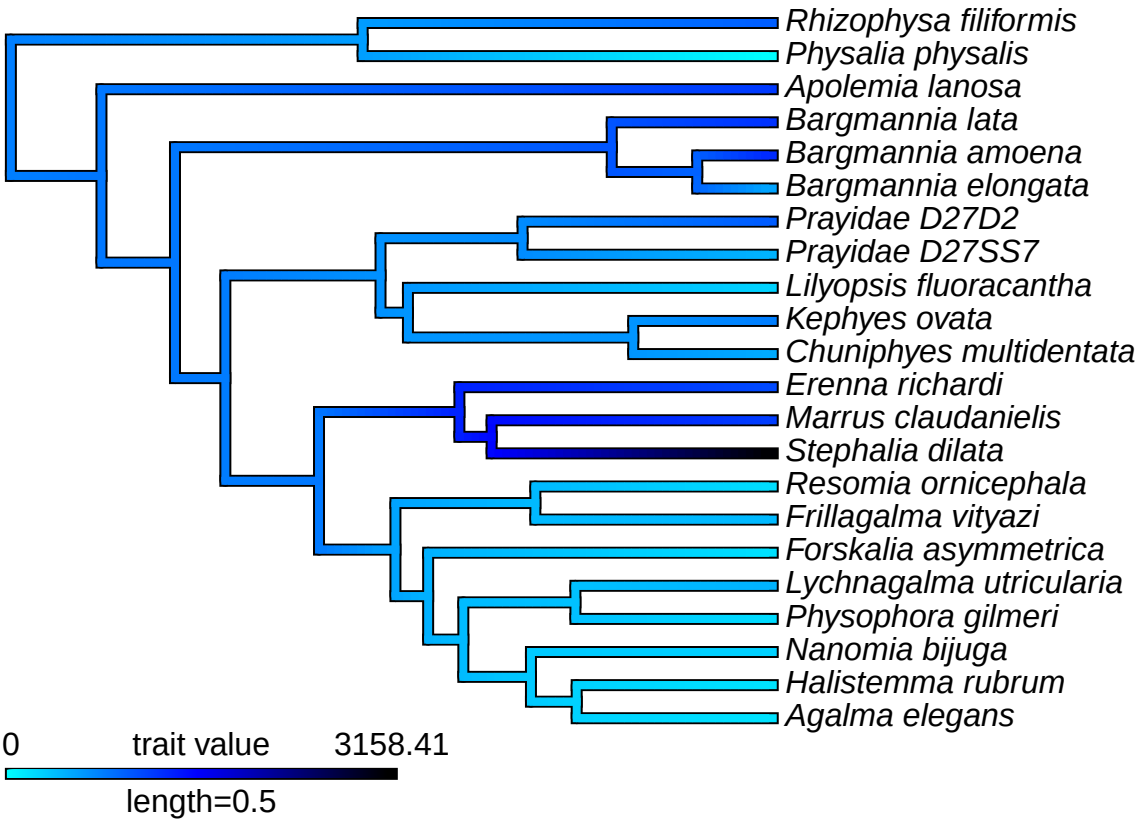

Bathymetrics phylomorphospace

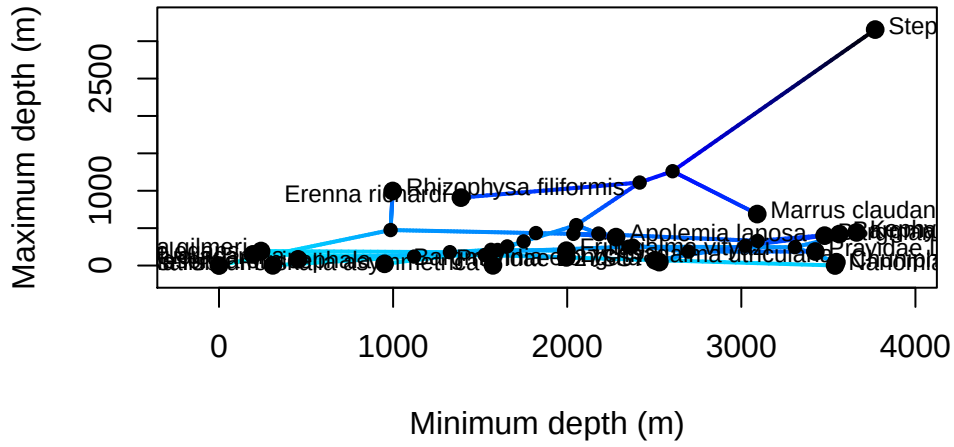

Bathymetrics phylomorphospace with time from root as color

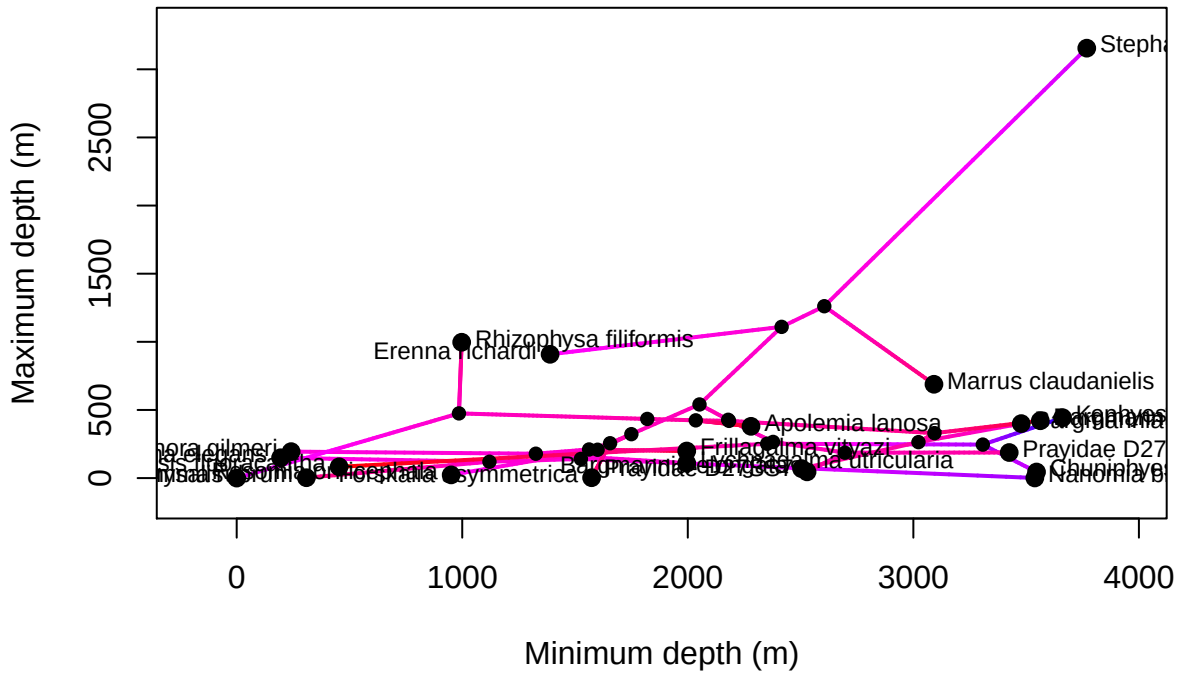

Abundance of each taxon in the Monterey Bay sampling site

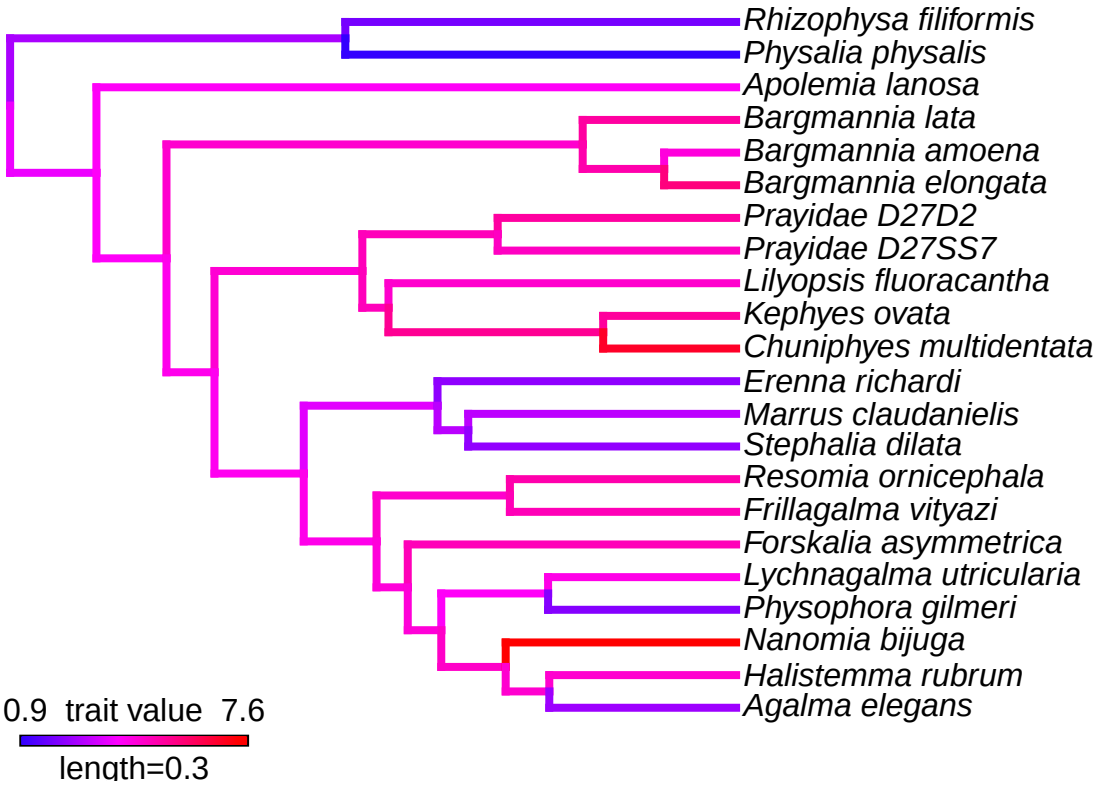

Uncertainty inclusive traitgram for depth range

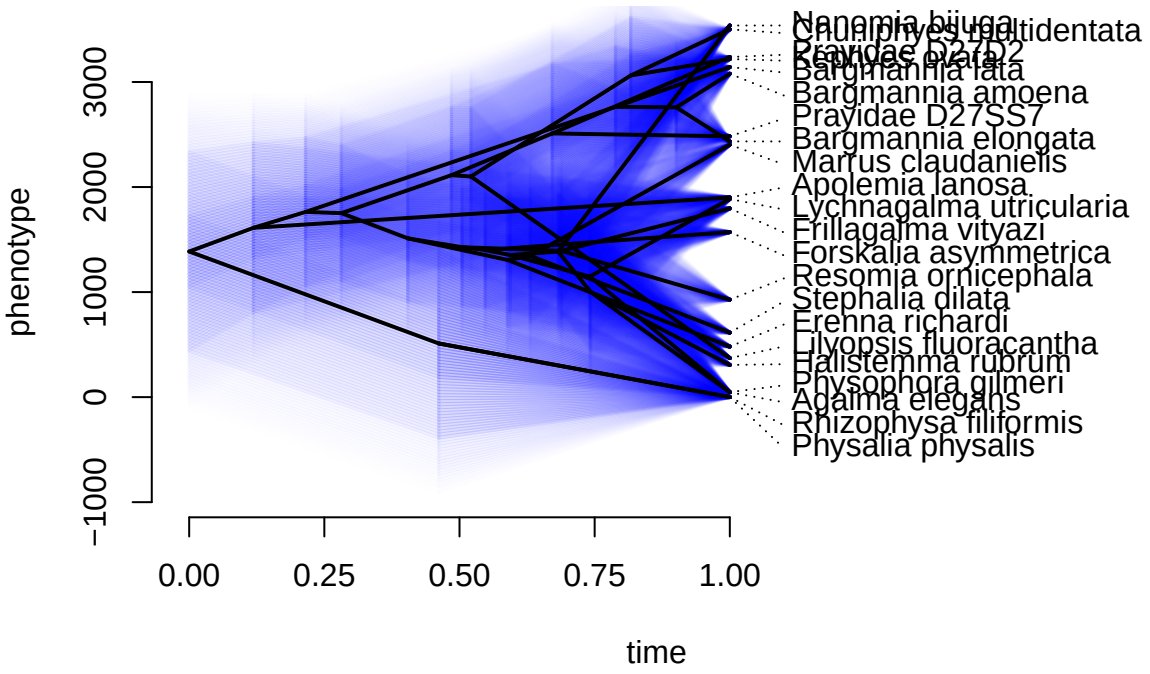

Bathymetrics scattergram array

```
## Computing multidimensional phylogenetic scatterplot matrix...
```

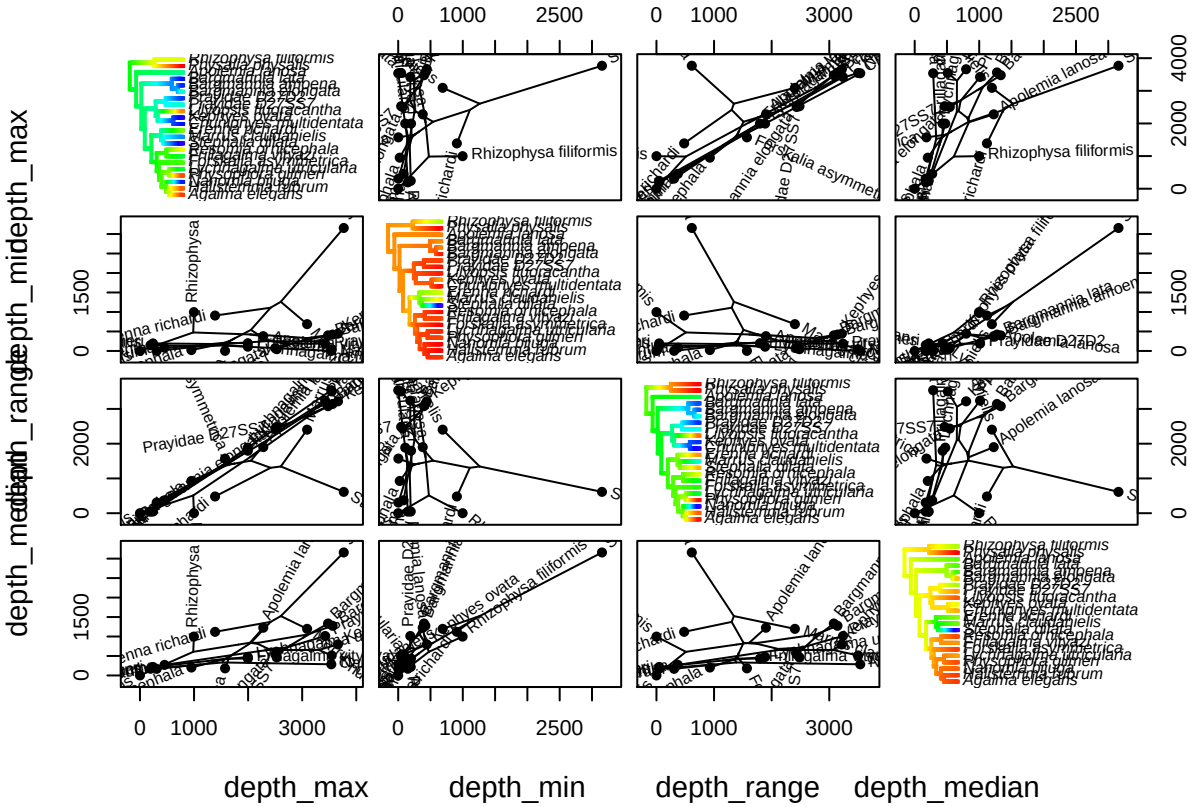

Distribution of sex across siphonophore taxa

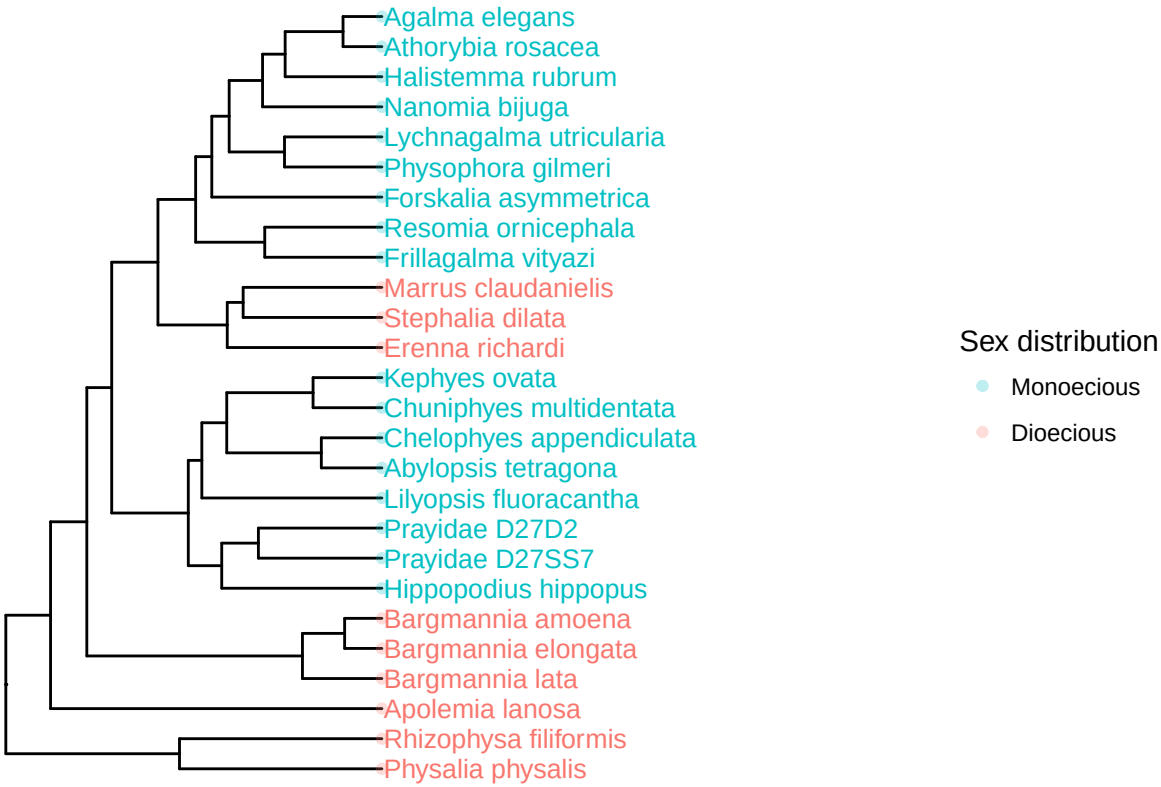

Tentilla presence across siphonophore taxa

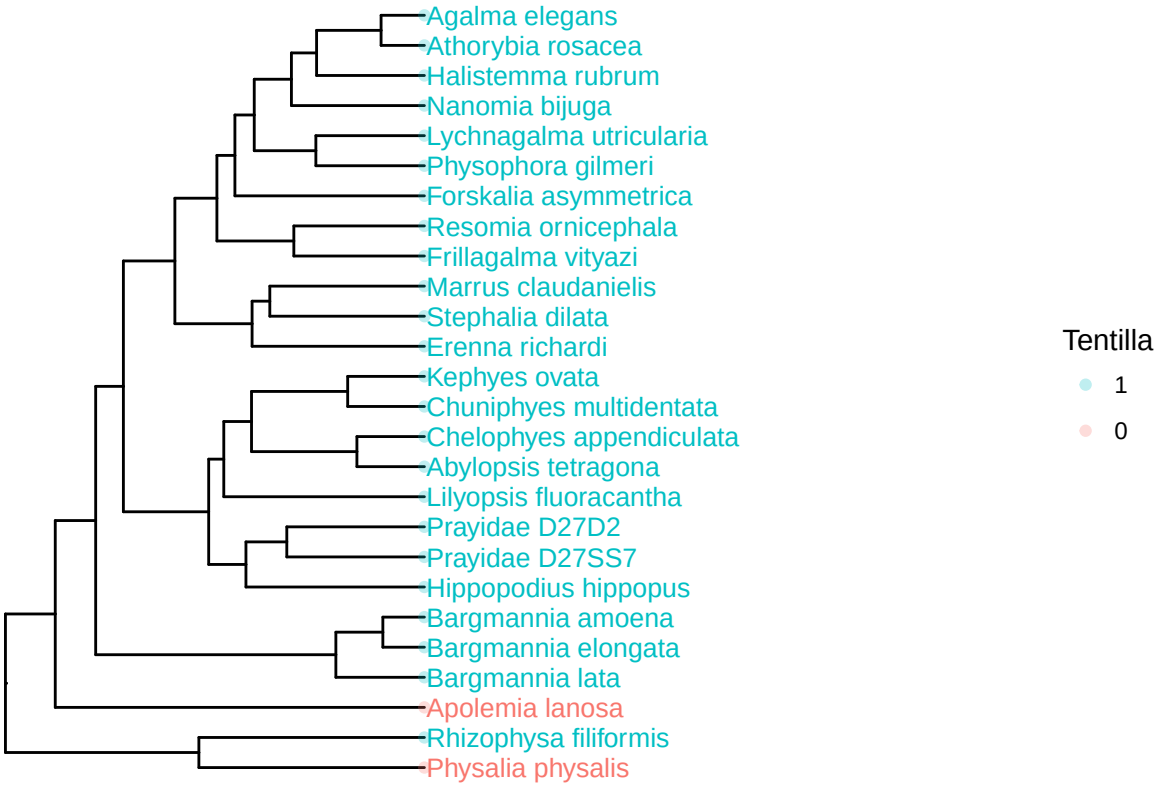

Palpon presence across siphonophore taxa

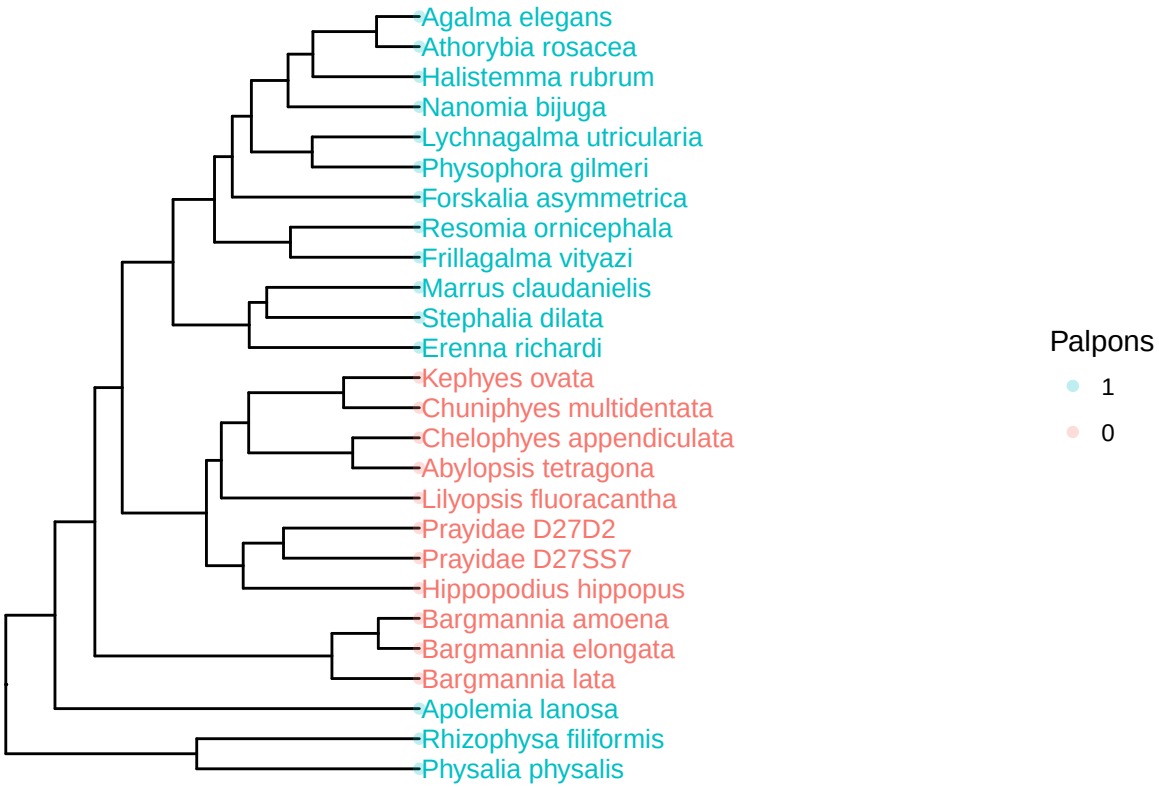

Overview grid of main binary traits

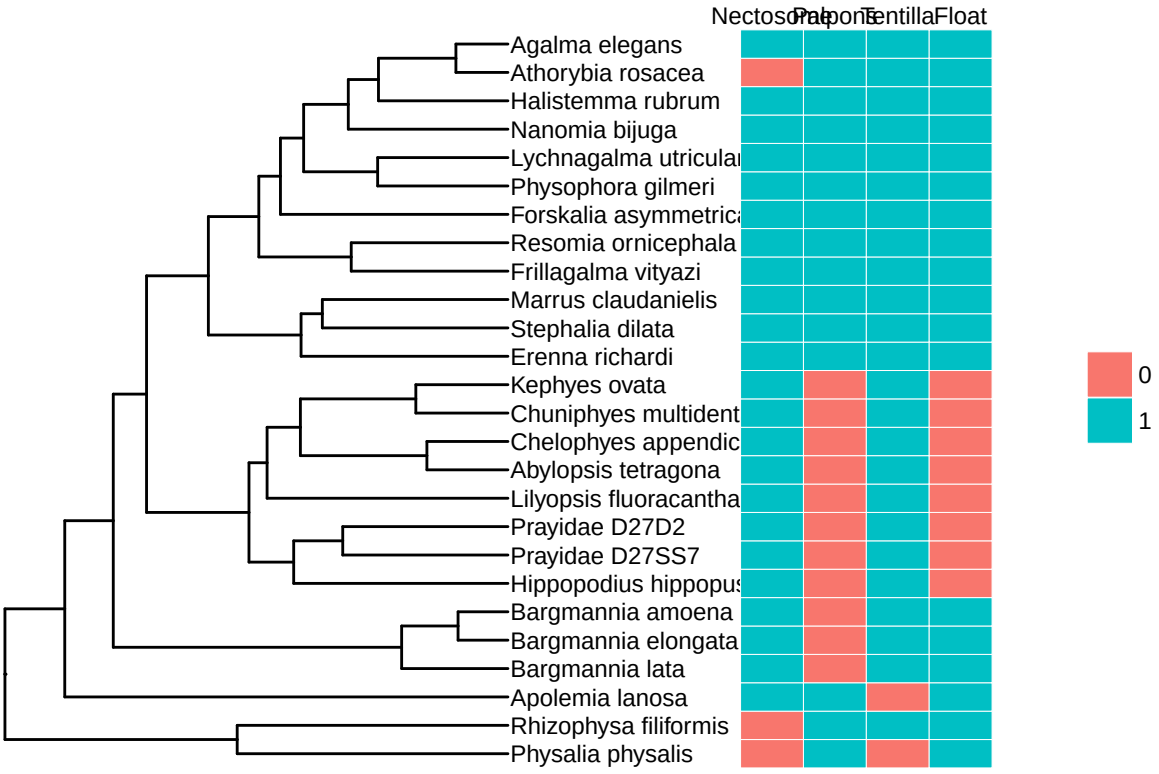

Phylogenetic signal in the character data

Agnostic branch length tree generation:

Phylogenetic signal in Binary Traits

```
##                       K PIC.variance.obs PIC.variance.rnd.mean
## Nectosome     0.6808842       0.27381627             0.3238316
## Palpons       3.1461479       0.10883086             0.7711969
## Tentilla      2.1089147       0.07847782             0.2228424
## Pneumatophore 3.3674883       0.09051674             0.6747076
##               PIC.variance.P PIC.variance.Z
## Nectosome             0.3655     -0.5165283
## Palpons               0.0010     -4.2649939
## Tentilla              0.0055     -1.7800034
## Pneumatophore         0.0010     -3.9776357
```

Phylogenetic signal in VARS bathymetrics

```
##
## Call:
## physignal(A = dpruned_data[, c(14, 15, 16, 18, 19)], phy = dpruned_tree)
##
##
##
##
## Observed Phylogenetic Signal (K): 0.713
##
## P-value: 0.041
##
## Based on 1000 random permutations
```

```
##                     K PIC.variance.obs PIC.variance.rnd.mean
## Depth.Median 0.7102056         874545.3               1315357
## Depth.Mean   0.6810206        1019335.8               1465471
## Depth.StdDev 0.5889906         137873.8                167099
## Depth.Max    0.7249934        3266103.9               4863631
## Depth.Min    0.7287560         828880.7               1284770
##              PIC.variance.P PIC.variance.Z
## Depth.Median          0.080     -1.0126409
## Depth.Mean            0.111     -0.9761313
## Depth.StdDev          0.223     -0.7610201
## Depth.Max             0.048     -1.5273666
## Depth.Min             0.129     -0.8671118
```

Phylogenetic PCA for bathymetrics

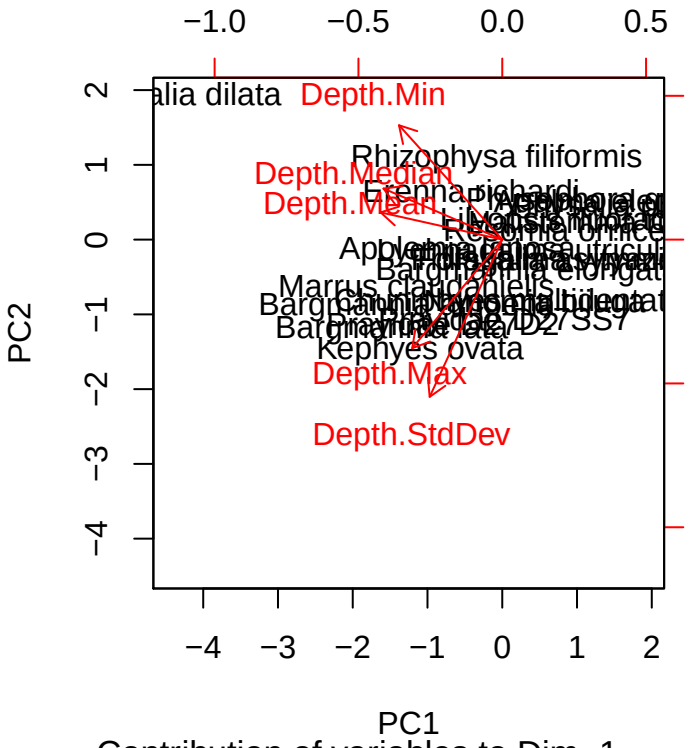
−1.0
−0.5
0.0
0.5
alia dilata
Depth.Min
Rhizophysa filiformis
Depth.Median
Depth.Mean
Marrus claudanielis
Kephyes ovata
Depth.Max
Depth.StdDev
PC2
PC1
2
1
0
−1
−2
−3
−4
0.5
0.0
−0.5
−1.0

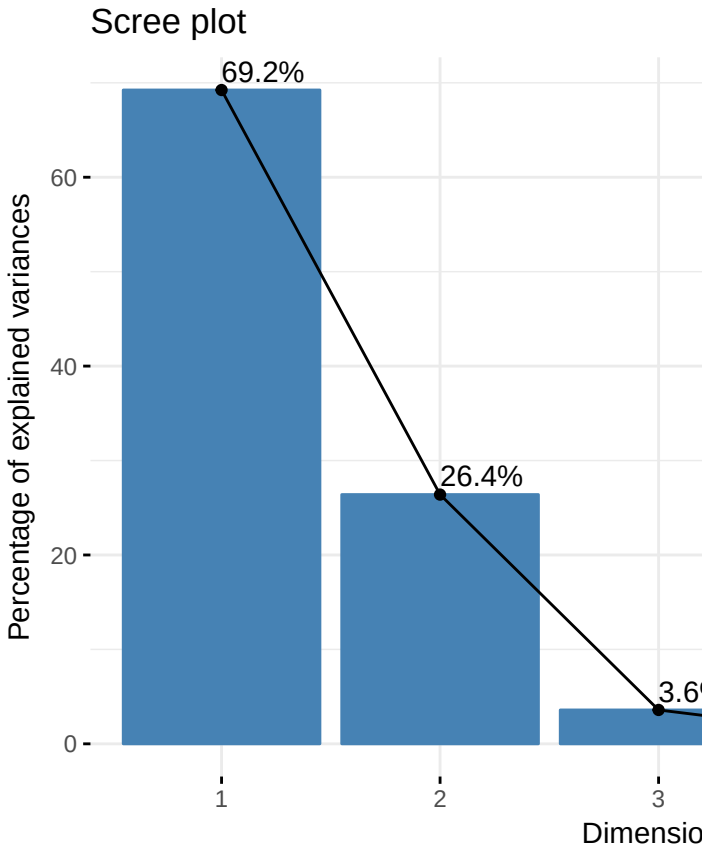
Scree plot
69.2%
26.4%
Percentage of explained variances
60
40
20
0
1
2
3
Dimensio

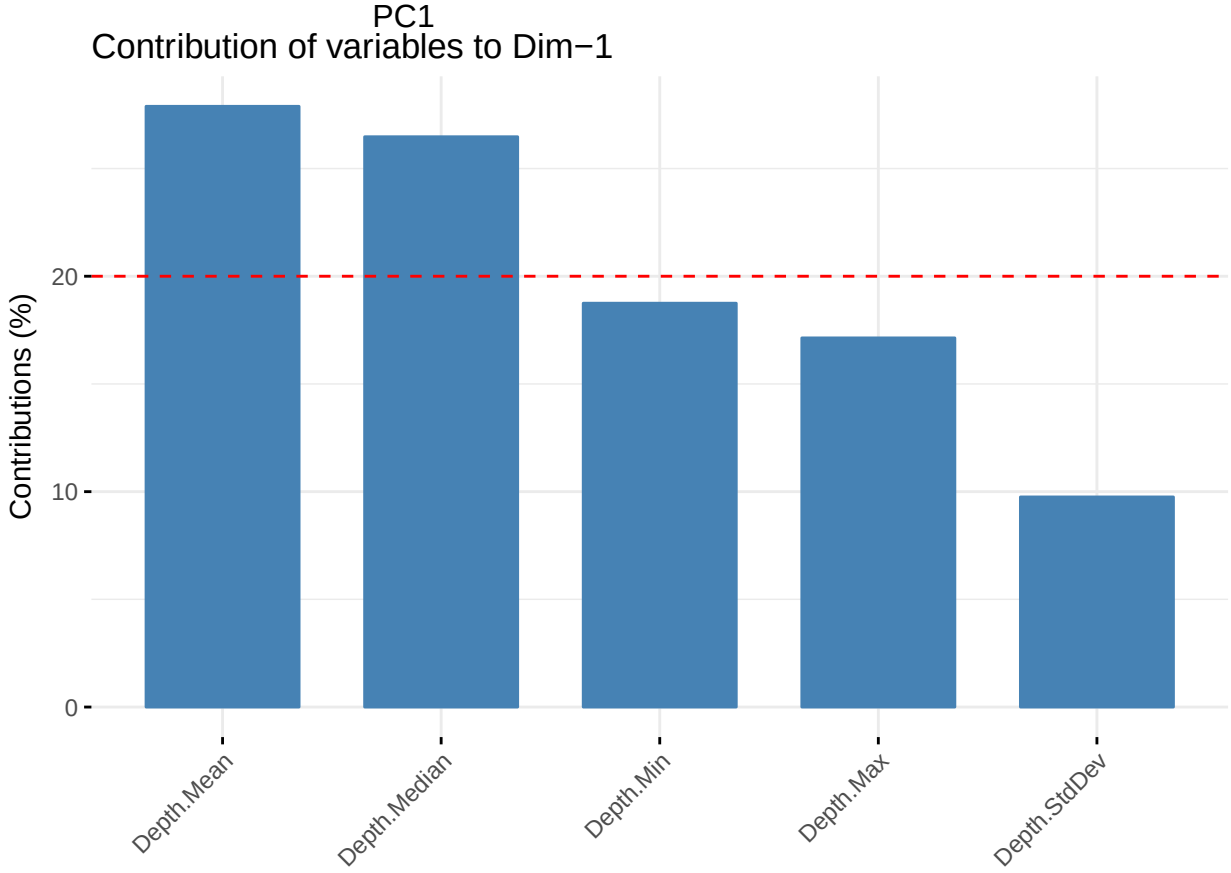
Contribution of variables to Dim−1
Contributions (%)
20
10
0
Depth.Mean
Depth.Median
Depth.Min
Depth.Max
Depth.StdDev

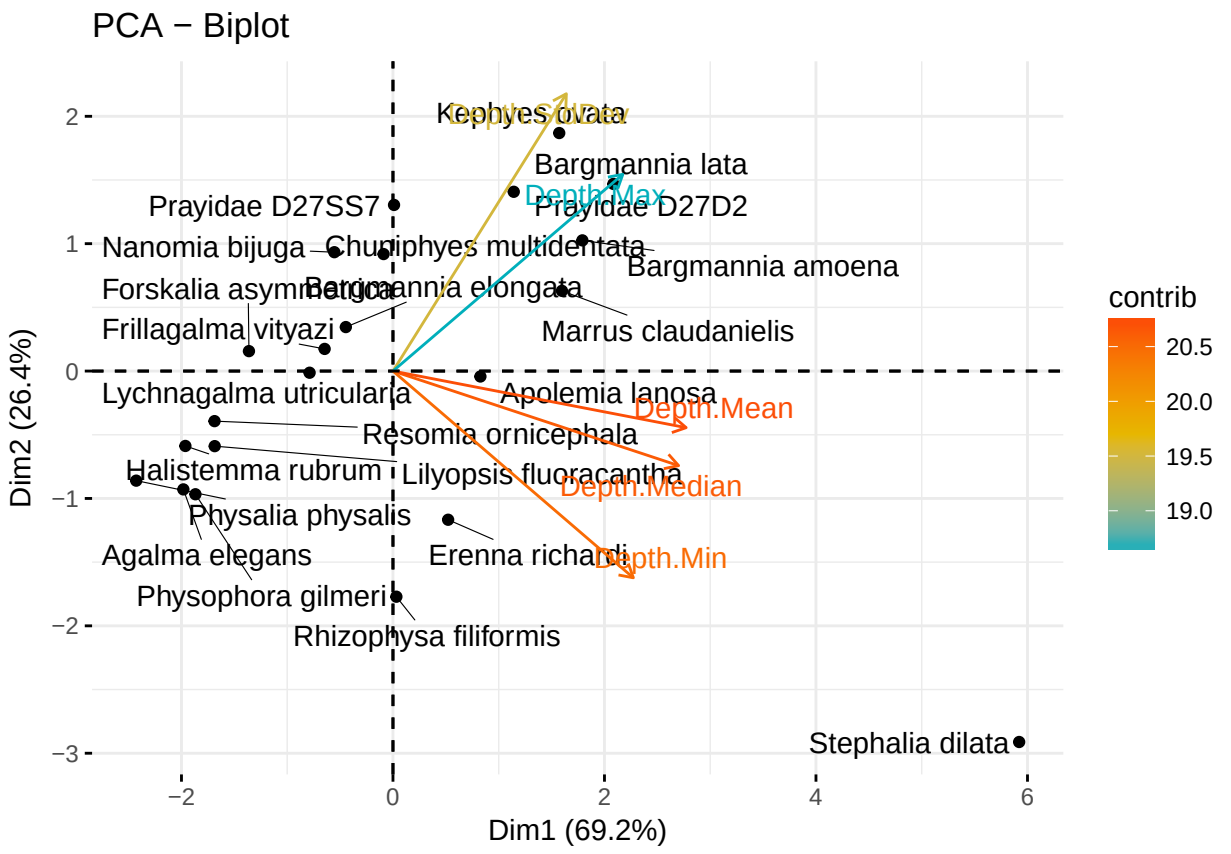
PCA − Biplot
Kephyes ovata
Bargmannia lata
Depth.Max
Prayidae D27SS7
Prayidae D27D2
Nanomia bijuga
Chuniphyes multidentata
Bargmannia amoena
Forskalia asymmetrica
Bargmannia elongata
Frillagalma vityazi
Marrus claudanielis
Lychnagalma utricularia
Apolemia lanosa
Depth.Mean
Resomia ornicephala
Halistemma rubrum
Lilyopsis fluoracantha
Depth.Median
Physalia physalis
Agalma elegans
Erenna richardi
Depth.Min
Physophora gilmeri
Rhizophysa filiformis
Stephalia dilata
contrib
20.5
20.0
19.5
19.0
Dim2 (26.4%)
Dim1 (69.2%)

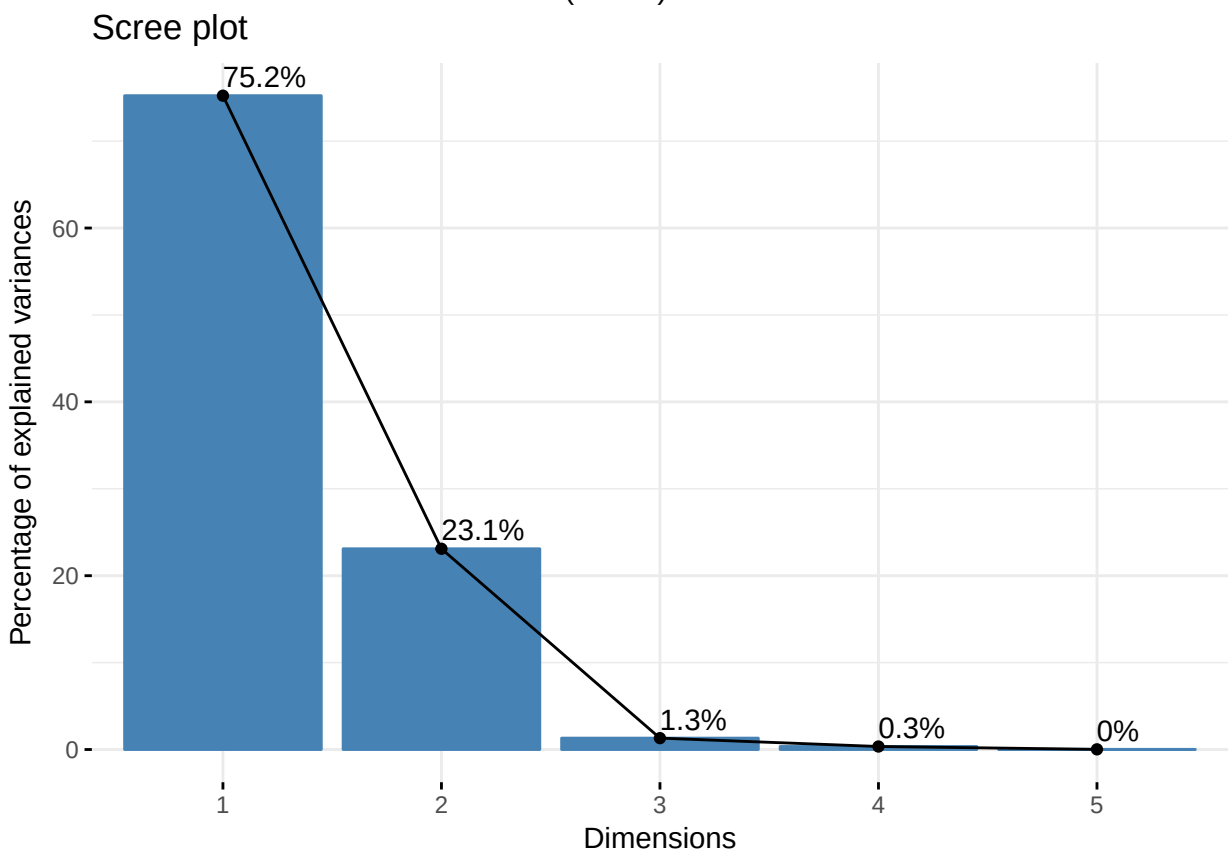
Scree plot
75.2%
23.1%
1.3%
0.3%
0%
Percentage of explained variances
Dimensions

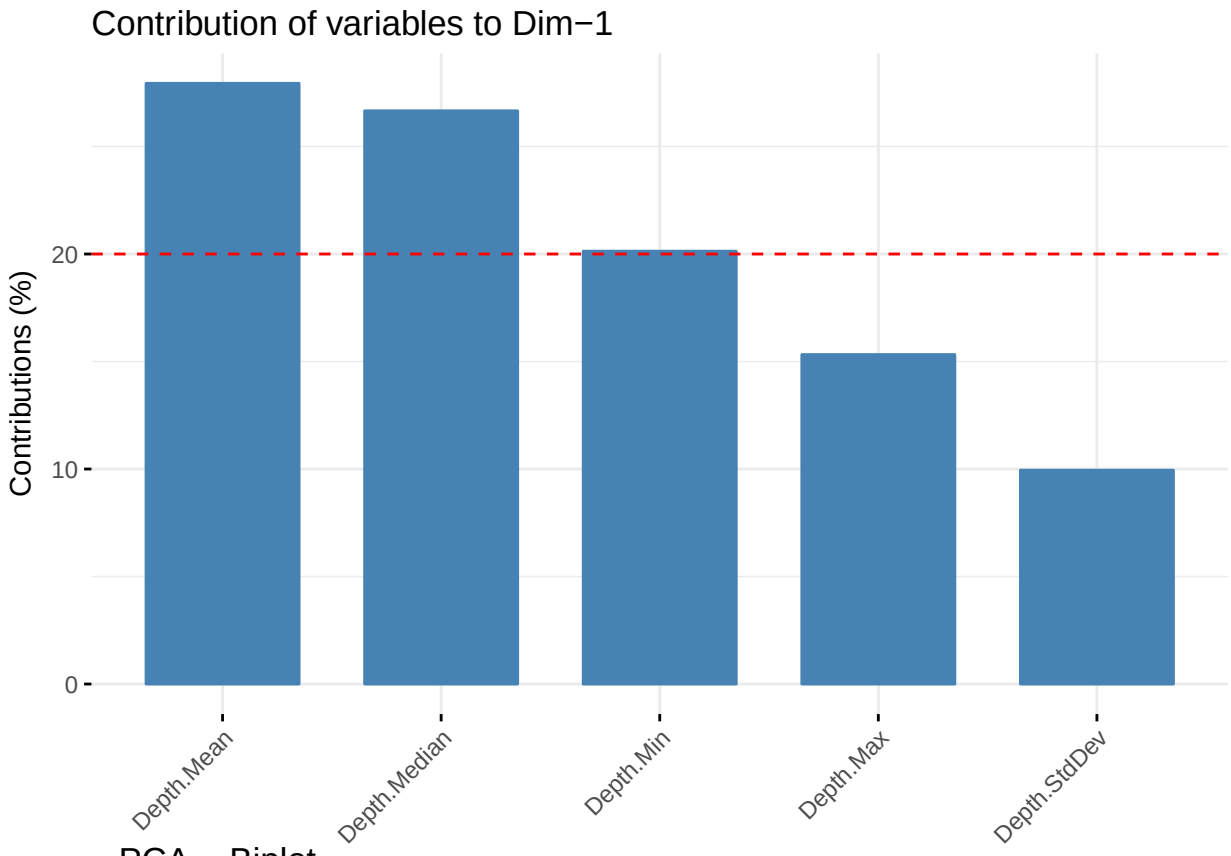
Contribution of variables to Dim−1
Contributions (%)
20
10
0
Depth.Mean
Depth.Median
Depth.Min
Depth.Max
Depth.StdDev

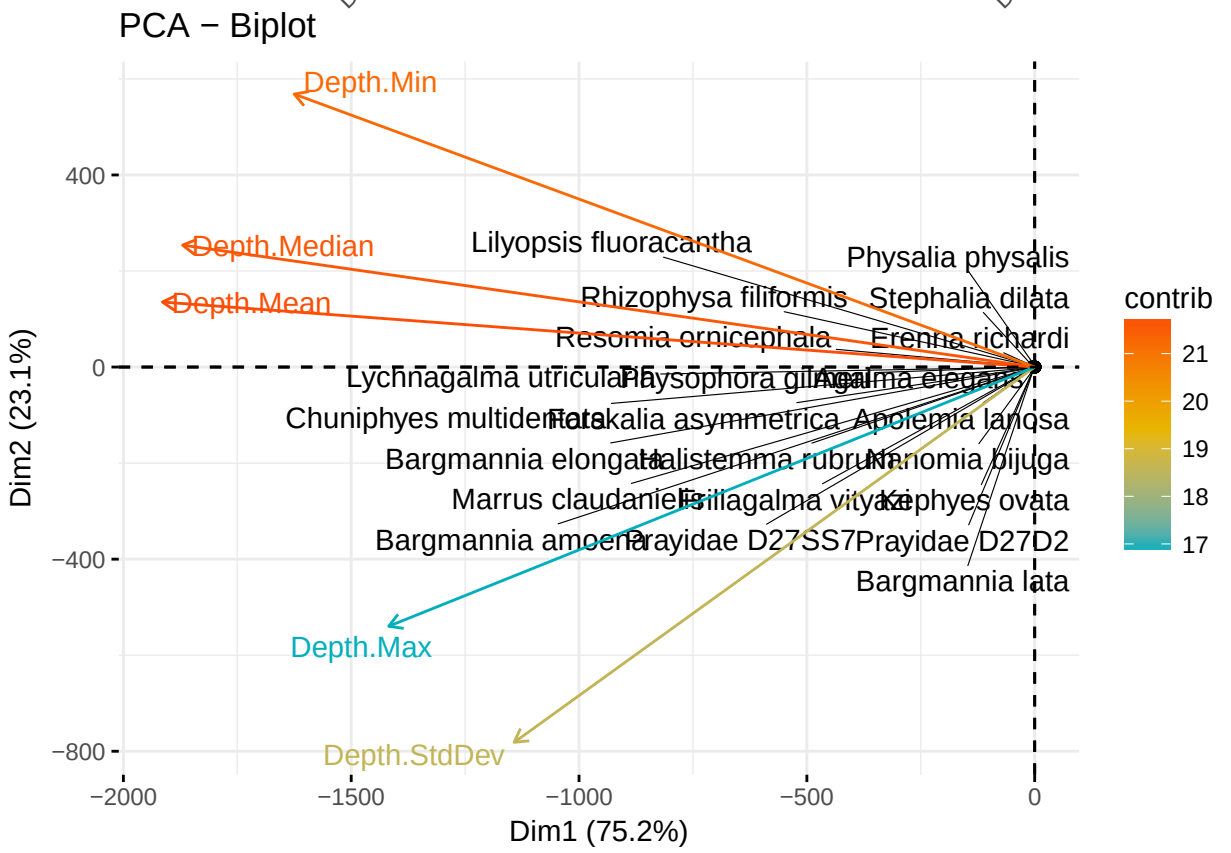
PCA − Biplot
Depth.Min
Depth.Median
Depth.Mean
Depth.Max
Depth.StdDev
Lilyopsis fluoracantha
Physalia physalis
Rhizophysa filiformis
Stephalia dilata
Resomia ornicephala
Erenna richardi
Lychnagalma utricularia
Physophora gilmeri
Agalma elegans
Chuniphyes multidentata
Forskalia asymmetrica
Apolemia lanosa
Bargmannia elongata
Halistemma rubrum
Marrus claudanielis
Nanomia bijuga
Bargmannia amoena
Prayidae D27SS7
Prayidae D27D2
Bargmannia lata
contrib
21
20
19
18
17
Dim2 (23.1%)
400
0
−400
−800
−2000
−1500
−1000
−500
0
Dim1 (75.2%)

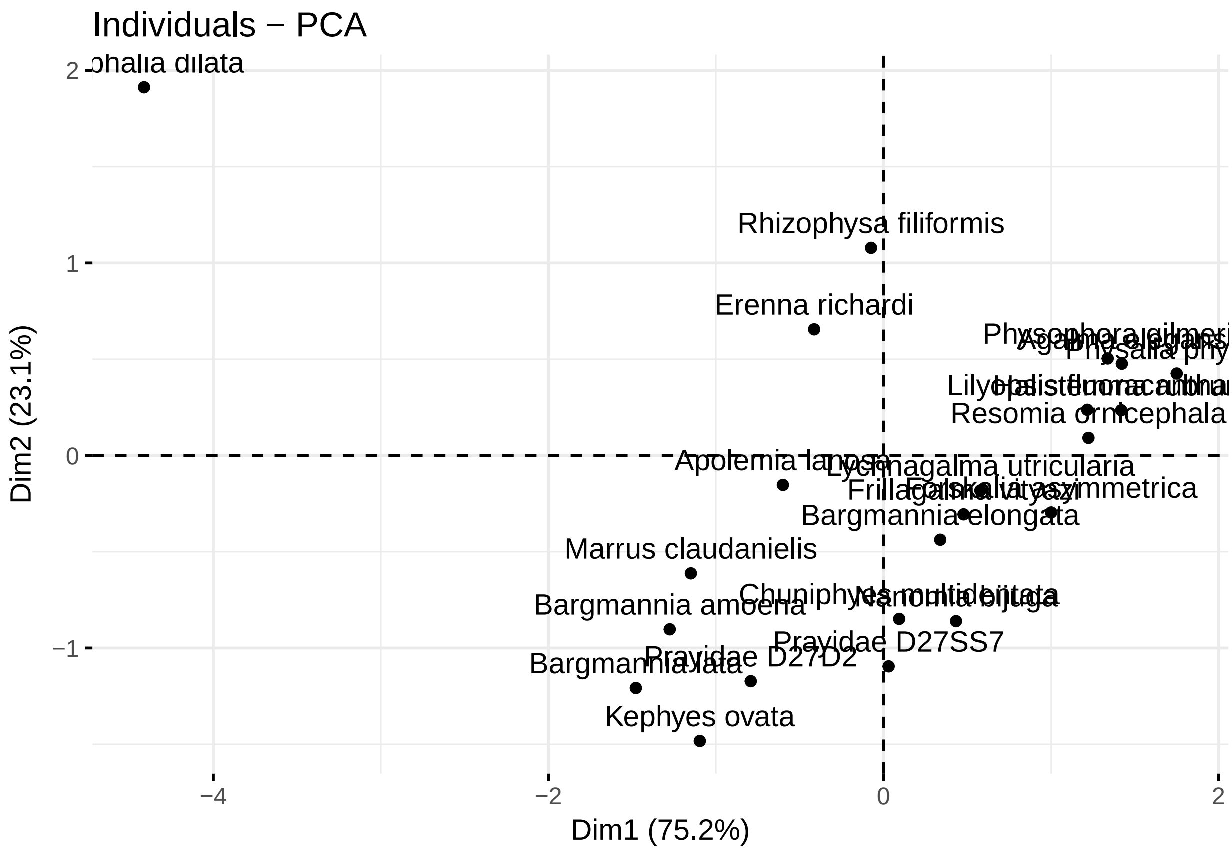

Phylogenetic ANOVA for depth

Each phylogenetic ANOVA compares variance of depth (continuous variable) within and between groups clustered by their categorical biological traits.

```
## [1] "Depth vs Sex Distribution"

## $F
## [1] 10.48139
##
## $Pf
## [1] 0.056
##
## $T
##            Dioecious Monoecious
## Dioecious   0.000000   3.237497
## Monoecious -3.237497   0.000000
##
## $method
## [1] "holm"
##
## $Pt
##            Dioecious Monoecious
## Dioecious      1.000      0.056
## Monoecious     0.056      1.000

## [1] "Depth vs Nectosome"
```

```
## $F
## [1] 0.2358588
##
## $Pf
## [1] 0.796
##
## $T
##          0         1
## 0 0.000000 -0.485653
## 1 0.485653  0.000000
##
## $method
## [1] "holm"
##
## $Pt
##       0     1
## 0 1.000 0.796
## 1 0.796 1.000
```

```
## [1] "Depth vs Nectophore Types and Number"
```

```
## $F
## [1] 0.156464
##
## $Pf
## [1] 0.98
##
## $T
##                       Multiple of one type None One of one type
## Multiple of one type                   NA   NA              NA
## None                                   NA   NA              NA
## One of one type                        NA   NA              NA
## Two of one type                        NA   NA              NA
## Two of two types                       NA   NA              NA
##                       Two of one type Two of two types
## Multiple of one type              NA               NA
## None                              NA               NA
## One of one type                   NA               NA
## Two of one type                   NA               NA
## Two of two types                  NA               NA
##
## $method
## [1] "holm"
##
## $Pt
##                       Multiple of one type None One of one type
## Multiple of one type                   NA   NA              NA
## None                                   NA   NA              NA
## One of one type                        NA   NA              NA
## Two of one type                        NA   NA              NA
## Two of two types                       NA   NA              NA
##                       Two of one type Two of two types
## Multiple of one type              NA               NA
## None                              NA               NA
## One of one type                   NA               NA
```

```
## Two of one type                   NA               NA
## Two of two types                  NA               NA
```

```
## [1] "Depth vs Nectosome Position"
```

```
## $F
## [1] 0.237949
##
## $Pf
## [1] 0.922
##
## $T
##             Dorsal      None    Ventral
## Dorsal   0.0000000 0.2240508 -0.4988957
## None    -0.2240508 0.0000000 -0.5640384
## Ventral  0.4988957 0.5640384  0.0000000
##
## $method
## [1] "holm"
##
## $Pt
##         Dorsal None Ventral
## Dorsal       1    1       1
## None         1    1       1
## Ventral      1    1       1
```

```
## [1] "Depth vs Palpons"
```

```
## $F
## [1] 0.05567054
##
## $Pf
## [1] 0.889
##
## $T
##            0         1
## 0  0.0000000 0.2359461
## 1 -0.2359461 0.0000000
##
## $method
## [1] "holm"
##
## $Pt
##       0     1
## 0 1.000 0.889
## 1 0.889 1.000
```

```
## [1] "Depth vs Tentilla"
```

```
## $F
## [1] 0.06009463
##
## $Pf
## [1] 0.873
##
## $T
##           0          1
```

```
## 0 0.0000000 -0.2451421
## 1 0.2451421  0.0000000
##
## $method
## [1] "holm"
##
## $Pt
##       0     1
## 0 1.000 0.873
## 1 0.873 1.000
```

```
## [1] "Depth vs Pneumatophore"
```

```
## $F
## [1] 0.1796993
##
## $Pf
## [1] 0.793
##
## $T
##           0          1
## 0 0.0000000 -0.4239096
## 1 0.4239096  0.0000000
##
## $method
## [1] "holm"
##
## $Pt
##       0     1
## 0 1.000 0.793
## 1 0.793 1.000
```

PGLS - Sex distribution

```
## ------------------------------------------------------------------
## | **Warning:                                                     |
## |   User reports suggest that this method may frequently      |
## |   fail to find the ML solution. Please use with caution.    |
## ------------------------------------------------------------------
```

```
## Call:
## phylolm(formula = depth_median ~ dp_sex, data = as.data.frame(cbind(depth_median,
##     dp_sex)), phy = dpruned_tree, model = "BM", measurement_error = TRUE,
##     boot = 100)
##
##    AIC logLik
##  347.8 -169.9
##
## Parameter estimate(s) using ML:
## sigma2: 0.04476443
## sigma2_error: 299475.5
##
## Coefficients:
## (Intercept)      dp_sex
##    399.7538    805.7584
```

```
## Generalized least squares fit by REML
##   Model: dp_sex ~ depth_median
##   Data: NULL
##   Log-restricted-likelihood: -20.52555
##
## Coefficients:
##  (Intercept) depth_median
## 0.0978229509 0.0004267556
##
## Degrees of freedom: 22 total; 20 residual
## Residual standard error: 0.4176998
```

Software versions

This manuscript was computed on Mon Oct 30 15:31:44 2017 with the following R package versions.

```
R version 3.4.1 (2017-06-30)
Platform: x86_64-apple-darwin15.6.0 (64-bit)
Running under: macOS Sierra 10.12.2

Matrix products: default
BLAS: /Library/Frameworks/R.framework/Versions/3.4/Resources/lib/libRblas.0.dylib
LAPACK: /Library/Frameworks/R.framework/Versions/3.4/Resources/lib/libRlapack.dylib

locale:
[1] en_GB.UTF-8/en_GB.UTF-8/en_GB.UTF-8/C/en_GB.UTF-8/en_GB.UTF-8

attached base packages:
[1] grid      parallel  stats     graphics  grDevices utils     datasets
[8] methods   base

other attached packages:
 [1] bindrcpp_0.2     phylolm_2.5      geomorph_3.0.5   rgl_0.98.1
 [5] adephylo_1.1-10  ade4_1.7-8       phylobase_0.8.4  geiger_2.0.6
 [9] phangorn_2.2.0   phytools_0.6-20  picante_1.6-2    nlme_3.1-131
[13] vegan_2.4-4      lattice_0.20-35  permute_0.9-4    ape_4.1
[17] hutan_0.5.0      FactoMineR_1.38  factoextra_1.0.5 gridExtra_2.3
[21] seriation_1.2-2  fields_9.0       maps_3.2.0       spam_2.1-1
[25] dotCall64_0.9-04 ggtree_1.8.2     treeio_1.0.2     cowplot_0.8.0
[29] xtable_1.8-2     jsonlite_1.5     knitr_1.17       digest_0.6.12
[33] magrittr_1.5     forcats_0.2.0    stringr_1.2.0    dplyr_0.7.4
[37] purrr_0.2.3      readr_1.1.1      tidyr_0.7.1      tibble_1.3.4
[41] ggplot2_2.2.1    tidyverse_1.1.1

loaded via a namespace (and not attached):
  [1] readxl_1.0.0            uuid_0.1-2
  [3] backports_1.1.1         fastmatch_1.1-0
  [5] plyr_1.8.4              igraph_1.1.2
  [7] lazyeval_0.2.0          sp_1.2-5
  [9] splines_3.4.1           rncl_0.8.2
 [11] foreach_1.4.3           htmltools_0.3.6
 [13] viridis_0.4.0           gdata_2.18.0
 [15] cluster_2.0.6           gclus_1.3.1
 [17] modelr_0.1.1            gmodels_2.16.2
```

```
 [19] prettyunits_1.0.2       jpeg_0.1-8
 [21] colorspace_1.3-2        rvest_0.3.2
 [23] ggrepel_0.7.0           haven_1.1.0
 [25] bindr_0.1               survival_2.41-3
 [27] iterators_1.0.8         glue_1.1.1
 [29] registry_0.3            gtable_0.2.0
 [31] seqinr_3.4-5            kernlab_0.9-25
 [33] prabclus_2.2-6          DEoptimR_1.0-8
 [35] scales_0.5.0            mvtnorm_1.0-6
 [37] DBI_0.7                 Rcpp_0.12.13
 [39] plotrix_3.6-6           viridisLite_0.2.0
 [41] progress_1.1.2          spdep_0.6-15
 [43] flashClust_1.01-2       foreign_0.8-69
 [45] subplex_1.4-1           bold_0.5.0
 [47] mclust_5.3              deSolve_1.20
 [49] stats4_3.4.1            animation_2.5
 [51] htmlwidgets_0.9         httr_1.3.1
 [53] gplots_3.0.1            fpc_2.1-10
 [55] modeltools_0.2-21       pkgconfig_2.0.1
 [57] reshape_0.8.7           XML_3.98-1.9
 [59] flexmix_2.3-14          deldir_0.1-14
 [61] nnet_7.3-12             crul_0.4.0
 [63] tidyselect_0.2.0        labeling_0.3
 [65] rlang_0.1.2             reshape2_1.4.2
 [67] munsell_0.4.3           cellranger_1.1.0
 [69] tools_3.4.1             broom_0.4.2
 [71] evaluate_0.10.1         yaml_2.1.14
 [73] robustbase_0.92-7       caTools_1.17.1
 [75] dendextend_1.5.2        mime_0.5
 [77] whisker_0.3-2           taxize_0.9.0
 [79] adegenet_2.1.0          leaps_3.0
 [81] xml2_1.1.1              compiler_3.4.1
 [83] curl_2.8.1              clusterGeneration_1.3.4
 [85] RNeXML_2.0.7            stringi_1.1.5
 [87] highr_0.6               trimcluster_0.1-2
 [89] Matrix_1.2-11           psych_1.7.8
 [91] msm_1.6.4               LearnBayes_2.15
 [93] combinat_0.0-8          data.table_1.10.4
 [95] bitops_1.0-6            httpuv_1.3.5
 [97] R6_2.2.2                TSP_1.1-5
 [99] KernSmooth_2.23-15      codetools_0.2-15
[101] boot_1.3-20             MASS_7.3-47
[103] gtools_3.5.0            assertthat_0.2.0
[105] rprojroot_1.2           mnormt_1.5-5
[107] diptest_0.75-7          mgcv_1.8-22
[109] expm_0.999-2            hms_0.3
[111] quadprog_1.5-5          coda_0.19-1
[113] class_7.3-14            rmarkdown_1.6
[115] rvcheck_0.0.9           ggpubr_0.1.5
[117] shiny_1.0.5             numDeriv_2016.8-1
[119] scatterplot3d_0.3-40    lubridate_1.6.0
```

References

Dunn C., Pugh P., Haddock S. 2005. Molecular Phylogenetics of the Siphonophora (Cnidaria), with Implications for the Evolution of Functional Specialization. Systematic biology. 54:916–935.

Dunn C.W., Howison M., Zapata F. 2013. Agalma: an automated phylogenomics workflow. BMC Bioinformatics. 14:330.

Lartillot N., Lepage T., Blanquart S. 2009. PhyloBayes 3: A bayesian software package for phylogenetic reconstruction and molecular dating. Bioinformatics. 25:2286–2288.

Lartillot N., Philippe H. 2004. A bayesian mixture model for across-site heterogeneities in the amino-acid replacement process. Molecular Biology and Evolution. 21:1095–1109.

Yu G., Smith D.K., Zhu H., Guan Y., Lam T.T.-Y. 2016. ggtree: an r package for visualization and annotation of phylogenetic trees with their covariates and other associated data. Methods in Ecology and Evolution.

Species	Mean insert size (bp)	Insert size standard deviation	Number of read pairs	Percent kept after rRNA removal	Percent kept after assembly	Adapter fails	Quality fails	Base Composition fails	Total assembled transcripts	Coding transcripts
Marrus claudanielis	253.03	53.30	35866092	96.8	62.1	113298	15594637	4981676	105439	22511
Apolemia rubriversa	290.81	80.64	19228660	91.7	77.8	40594	5179800	516100	87701	17540
Chuniphyes multidentata	284.46	35.74	17999147	77.0	74.3	24263	4941872	335297	84341	22084
Apolemia sp	167.41	53.46	16761717	81.3	79.4	1332063	3062035	41943	51470	14752
Apolemia lanosa	167.74	55.30	18444476	96.4	80.9	923922	3882968	439569	70184	15579
Bargmannia elongata	271.43	40.17	40008913	79.8	78.5	342825	8084832	2017709	152019	23661
Diphyes dispar	223.14	58.73	80000000	78.7	63.4	14412120	21322624	690159	210406	50868
Aiptasia pallida	183.18	53.88	74558341	98.4	79.3	210730	23826421	307520	83950	33523
Stephalia dilata	267.82	43.33	30953585	98.0	63.9	86068	15731787	1435119	107925	23984
Physalia physalis	233.10	54.37	36481773	96.6	88.5	18553	5491979	259497	74994	23705
Bargmannia amoena	161.57	53.77	20195498	84.6	80.1	1049110	3996085	274520	66726	17975
Frillagalma vityazi	283.11	44.91	79902051	54.0	70.4	668400	13591301	5558767	181508	29293
Alatina alata	173.96	60.33	96259870	52.1	77.9	1236251	15771112	468662	166584	28743
Clytia hemisphaerica									11476	6642
Ectopleura larynx	229.05	37.75	109024653	95.9	74.6	432309	40629127	897590	84034	28015
Athorybia rosacea	221.16	93.65	28696930	99.9	86.9	691916	4026467	633700	100839	24543
Forskalia asymmetrica	259.42	35.04	25275184	58.9	65.1	41922	7463840	841930	82483	18419
Prayidae D27D2	267.32	45.59	38233199	85.2	66.4	59773	15338562	1878732	144909	28065
Lilyopsis fluoracantha	259.39	39.08	51855968	76.5	65.3	72416	19809124	1388875	114662	29854
Hydractinia symbiolongicarpus	175.22	57.84	60462724	49.8	85.2	162430	6678373	124392	71450	24639
Rhizophysa filiformis	269.74	46.52	26937827	92.5	65.3	66010	13238701	361376	110109	24833
Agalma elegans	238.94	57.54	40007833	99.6	86.0	31957	7177806	748977	122053	26601
Chelophyes appendiculata	275.93	39.43	21103284	89.0	74.2	63548	6777022	344708	110612	32309
Prayidae D27SS7	303.39	50.83	25233164	66.7	65.6	39061	8616289	347189	94917	24211
Rudjakovia sp	213.88	89.71	20582477	99.1	79.7	489520	3936086	1546686	91695	24184
Abylopsis tetragona	292.16	38.32	21575176	73.3	73.8	38764	5759144	370604	102946	25268
Nematostella vectensis									26511	18080
Hippopodius hippopus	266.99	45.11	35638254	84.5	66.3	56152	15490291	535026	137341	35031
Physophora gilmeri	214.97	93.78	19847377	99.3	81.3	936617	3464079	1007839	52639	17381
Bargmannia lata	166.71	62.80	16984483	98.7	71.1	3118496	4227140	868584	59051	16451
Nanomia bijuga	296.69	44.20	39983229	85.7	75.3	155093	10854240	795226	165792	28927
Erenna richardi	291.53	36.76	29776547	64.2	66.6	39775	8958200	1245523	89423	18236
Physonect sp	261.09	35.96	38243543	24.3	66.7	12494	4517982	274838	57746	12596